13920–13938 *Nucleic Acids Research, 2014, Vol. 42, No. 22* *Published online 26 November 2014*
doi: 10.1093/nar/gku1132

Drosophila melanogaster LRPPRC2 is involved in coordination of mitochondrial translation

Francesca Baggio[1], Ana Bratic[1], Arnaud Mourier[1], Timo E.S. Kauppila[1], Luke S. Tain[2], Christian Kukat[1,3], Bianca Habermann[4], Linda Partridge[2] and Nils-Göran Larsson[1,5,*]

[1]Department of Mitochondrial Biology, Max Planck Institute for Biology of Ageing, Cologne 50931, Germany, [2]Department of the Biological Mechanisms of Ageing, Max Planck Institute for Biology of Ageing, Cologne 50931, Germany, [3]FACS & Imaging Core Facility, Max Planck Institute for Biology of Ageing, Cologne 50931, Germany, [4]Department of Computational Biology, Max Planck Institute of Biochemistry, Martinsried 82152, Germany and [5]Department of Laboratory Medicine, Karolinska Institutet, Stockholm 17177, Sweden

Received January 23, 2014; Revised October 20, 2014; Accepted October 25, 2014

ABSTRACT

Members of the pentatricopeptide repeat domain (PPR) protein family bind RNA and are important for post-transcriptional control of organelle gene expression in unicellular eukaryotes, metazoans and plants. They also have a role in human pathology, as mutations in the leucine-rich PPR-containing (*LRPPRC*) gene cause severe neurodegeneration. We have previously shown that the mammalian LRPPRC protein and its *Drosophila melanogaster* homolog DmLRPPRC1 (also known as bicoid stability factor) are necessary for mitochondrial translation by controlling stability and polyadenylation of mRNAs. We here report characterization of DmLRPPRC2, a second fruit fly homolog of LRPPRC, and show that it has a predominant mitochondrial localization and interacts with a stem-loop interacting RNA binding protein (DmSLIRP2). Ubiquitous downregulation of *DmLrpprc2* expression causes respiratory chain dysfunction, developmental delay and shortened lifespan. Unexpectedly, decreased DmLRPPRC2 expression does not globally affect steady-state levels or polyadenylation of mitochondrial transcripts. However, some mitochondrial transcripts abnormally associate with the mitochondrial ribosomes and some products are dramatically overproduced and other ones decreased, which, in turn, results in severe deficiency of respiratory chain complexes. The function of DmLRPPRC2 thus seems to be to ensure that mitochondrial transcripts are presented to the mitochondrial ribosomes in an orderly fashion to avoid poorly coordinated translation.

INTRODUCTION

The mitochondrial DNA (mtDNA) of *Drosophila melanogaster* is a ∼19.5-kb circular molecule containing 37 genes. The gene content is conserved between fly and mammalian mtDNA, but the gene order is different. As in mammals, fly mtDNA encodes 11 mRNAs, translated to 13 polypeptides that all are oxidative phosphorylation (OXPHOS) complex subunits, 2 rRNAs and 22 tRNAs (1,2). The regulation of mtDNA expression is dependent on hundreds of nucleus-encoded factors operating at different levels to regulate genome maintenance, transcription and post-transcriptional events like RNA processing, RNA modification, RNA stability and translation regulation (3,4). These processes are incompletely understood but we have previously shown that key regulatory post-transcriptional processes and factors often are conserved between flies and mammals (5–7).

The pentatricopeptide repeat domain (PPR) protein family was first discovered by an *in silico* approach in plants (8) and all members are predicted to be imported into mitochondria and/or chloroplasts. The PPR proteins are not only present in plants but have also been identified in mitochondria of yeast, protozoa and metazoa (9,10). The PPR family is subdivided into two major classes, P and PLS (11). The P-class proteins contain tandem arrays of the canonical 35-amino-acid PPR motif (P), whereas the PLS-class proteins contain tandem arrays of triplet repeats consisting of a canonical PPR motif (P), a slightly longer PPR motif (L) and a slightly shorter PPR motif (S) (11–15). The P-class proteins have been reported to regulate post-transcriptional processes, such as RNA stability, RNA degradation, RNA processing, RNA modification and mitochondrial translation (9,14). The vast majority of the PLS-class proteins is expressed in land plants and is mainly involved in RNA editing (10,16).

*To whom correspondence should be addressed. Tel: +49 221 37970 700; Fax: +49 22 37970 800; Email: larsson@age.mpg.de

The modular 35-amino-acid sequence repeated in tandem in canonical P motifs is characterized by high affinity for interactions with RNA (8,9,15). The binding to RNA is determined by amino acids located in specific positions of each P motif, defining a molecular code which establishes the modality of RNA recognition by PPR proteins (17–21). Recent structural work has shown that each P motif forms a hairpin of two antiparallel α-helices connected by a short turn of two amino acids (20). Each α-helix is composed of four helical turns followed by a five-amino-acid loop (20).

Plants often have several hundred different PPR proteins, e.g. ∼450 different ones are found in *Arabidopsis* (11). Surprisingly, the number of PPR proteins is much smaller in other organisms, e.g. there are 15 in *Saccharomyces cerevisiae*, 10 in *Schizosaccharomyces pombe* (22), 39 in the protozoan *Trypanosoma brucei* (23) and 7 in mammals (9,24,25). The mammalian PPR proteins include the mitochondrial RNA polymerase (POLRMT) (26), the PPR domain-containing protein 1 (PTCD1) (27,28), PTCD2 (29), PTCD3 (30), the mitochondrial ribosomal protein S27 (MRPS27) (31), the mitochondrial ribonuclease P protein 3 (MRPP3) (32) and the leucine-rich PPR-containing protein (LRPPRC, also named LRP130) (7,33–37). The mammalian LRPPRC protein is of particular interest because a recessive mutation in its gene causes a severe neurodegenerative disease called Leigh syndrome French Canadian variant (38–40). In *Drosophila melanogaster*, the PPR proteins are poorly characterized and Flybase (http://flybase.org) contains 7 annotated putative PPR proteins. They are all homologs of the mammalian PPR proteins, but there is as yet no identified fly homolog of the mammalian PTCD2. Surprisingly, flies contain two LRPPRC homologs (6,33) that we have named DmLRPPRC1, previously known as bicoid stability factor (6), and DmLRPPRC2 (annotation number #CG14786). We have previously shown that mammalian LRPPRC (7) and fly DmLRPPRC1 (6) have very similar functions in mitochondria where they control mRNA stability, polyadenylation and mitochondrial translation.

In this study, we have investigated the *in vivo* role of DmLRPPRC2 to determine whether it has distinct or overlapping functions with respect to those of DmLRPPRC1. We show that DmLRPPRC2 is a mitochondrial protein that interacts with DmSLIRP2 and is essential for mtDNA expression and oxidative phosphorylation. Downregulation of DmLRPPRC2 causes delayed larval development, neuromuscular phenotypes and shortened lifespan in adult flies. Surprisingly, unlike DmLRPPRC1 and LRPPRC, DmLRPPRC2 is not involved in regulating mRNA stability or polyadenylation, but it seems to be necessary for proper coordination of mitochondrial translation. Our results show that DmLRPPRC1 and DmLRPPRC2 have distinct essential roles in the regulation of mtDNA expression.

MATERIALS AND METHODS

Drosophila stocks and maintenance

All fly stocks were maintained at 25°C on a standard agar-yeast-sucrose medium under constant humidity and 12 h:12 h light:dark cycle. For the knockdown (KD) studies, two independent UAS-*Lrpprc2* RNAi lines were used: w;UAS-*Lrpprc2*RNAi#1 (#NM_130557.2) was purchased from the National Institute of Genetics (NIG, Japan) and w;;UAS-*Lrpprc2*RNAi#2 (#v42899) was purchased from the Vienna *Drosophila* RNAi Center (VDRC, Austria). Ubiquitous *DmLrpprc2* KD was achieved by crossing UAS-*Lrpprc2* RNAi lines with a *daughterless*-GAL4 (*da*GAL4) driver line. All fly lines were backcrossed for at least six generations into the *white Dahomey* background (*wDahT*) that is free from the endosymbiontic bacterium *Wolbachia*.

Eclosion rate, climbing and lifespan analyses

To determine the eclosion rates of KD and control lines, 1500–2000 embryos were collected after 4 h of egg laying. Embryos were distributed in a density of 100 per vial containing standard agar-yeast-sucrose medium. Eclosion rates, which represent the percentage of eclosed pupae with respect to the total number of collected embryos, were calculated relative to the eclosion rates of the control line w;;*da*GAL4/+.

The climbing assay was performed as described in (41). Briefly, 13-day-old males were used to determine the locomotor and negative geotaxis behavior of KD and control lines. A total of 130–300 males were divided into groups of ∼25 males and placed in plastic tubes without food. The experiments were executed after 2 h to allow proper CO_2-anesthesia recovery.

For lifespan studies, 130–200 females were collected immediately after eclosion and mated for 1 day. Females were distributed at a density of 10 flies per vial.

All assays were performed at 25°C.

Imaging and colocalization analyses

The UT01249 clone containing the full-length *Drosophila melanogaster Lrpprc2* cDNA sequence was purchased from the *Drosophila* Gene Collection (DGC) of Berkeley *Drosophila* Genome Project (BDGP). At variance with the annotated reference sequence FBgn0027794 reported in Flybase (http://flybase.org), we found two non-synonymous mutations (C835G and T2783C). In order to recreate the original sequence, both mutations were changed by using the QuickChange II XL Site-Directed Mutagenesis Kit (Agilent Technologies). Next, the *DmLrpprc2* cDNA sequence was cloned into the pAcGFP1-N3 vector (Clontech). The obtained plasmid pDmLRPPRC2-GFP was transfected to HeLa cells to express the chimeric protein composed of DmLRPPRC2 fused in frame at its carboxy-terminus with green fluorescent protein (AcGFP1). Transfection was done in microscopy dishes (μ-Slide, ibidi) by means of FuGENE HD Transfection Reagent (Roche Diagnostics). To visualize the mitochondrial network, HeLa cells were stained with the mitochondrial marker MitoTracker Deep Red FM (Invitrogen). A Leica TCS SP5-X confocal microscope (Leica Microsystems) was used for image acquisition. The colocalization rate between the DmLRPPRC2-GFP and MitoTracker signals was determined using the LAS AF software (Leica Microsystems) under conditions of 30% threshold and 20% background, applying the following formula: colocalization rate [%] =

colocalization area/area foreground, and area foreground = area image − area background. Oligonucleotide primers used for cloning are reported in Table 1.

Western blot analyses

Western blot experiments were performed as described in the Cell Signaling Technology protocol (CellSignaling) on whole-body or isolated mitochondrial protein extracts from third-instar larvae or 6-day-old adults. Briefly, 10 larvae/flies were homogenized on ice in a cold RIPA buffer (50 mM Tris-HCl pH 7.5, 150 mM NaCl, 1 mM ethylenediaminetetraacetic acid (EDTA)), supplemented with EDTA-free complete protease inhibitor cocktail (Roche). Bradford assays were performed to assess protein concentrations. Protein extracts, 20–40 μg, were denatured at 95°C for 5 min and separated in 4–20% Criterion Tris-HCl precast sodium dodecyl sulphate-polyacrylamide gel electrophoresis (SDS-PAGE) gels (Bio-Rad). After electrophoresis, proteins were transferred to Hybond-P polyvinylidene difluoride (PVDF) membranes (GE Healthcare). The used primary antibodies were: Complex I-subunit NDUFS3 (Mitoscience MS112, dilution 1:1000), Complex V-subunit ATP5A (Abcam ab14748, dilution 1:5000), VDAC (Abcam Ab14734, dilution 1:2000), a polyclonal rabbit antiserum raised against DmLRPPRC2 (generated by Peptide Specialty Laboratories (PSL) GmbH, dilution 1:1000), a polyclonal rat antiserum raised against DmLRPPRC1 (kindly provided by Professor MacDonald PM, Stanford University, dilution 1:1000). After incubation of the membrane with peroxidase-conjugated secondary antibodies (GE Healthcare), immunodetection was performed using enhanced chemiluminescence kit (Immun-Star HRP Luminol/Enhancer Bio-Rad).

Subcellular fractionation

Subcellular fractionation experiments were performed according to (42), with slight modifications. Approximately 2 ml adult wDahT flies were homogenized in a cold 250-STMDPS buffer (250 mM sucrose, 50 mM Tris-HCl pH 7.4, 5 mM $MgCl_2$, 1 mM dithiothreitol (DTT), 25 mg/ml Spermine, 25 mg/ml Spermidine, 1 mM phenylmethylsulfonyl fluoride (PMSF), 0.1% bovine serum albumin (BSA)). In order to remove the fly legs and wing debris, the homogenate was sieved through a 100 μm cell strainer (BD Falcon). Afterwards, mitochondrial, cytoplasmic and nuclear fractions were separated by differential centrifugation. All isolated fractions were separated in 4–15% Criterion Tris-HCl precast SDS-PAGE gels (Bio-Rad) and tested by a standard western blotting procedure. Each fraction was tested with the following primary antibodies: histone H3 (Sigma, dilution 1:200), VDAC (Mitosciences MSA03, dilution 1:1000), tubulin (Sigma, dilution 1:1000) and a polyclonal rabbit antiserum raised against DmLRPPRC2 (generated by PSL GmbH, dilution 1:1000).

Isolation of mitochondria

Approximately 6 ml of third-instar larvae and 2 ml of 6-day-old adults were washed and homogenized into 15 ml Dounce homogenizers in ice-cold Mitochondria Isolation Buffer STE + BSA (250 mM sucrose, 5 mM Tris, 2 mM EGTA, 1% (w/v) fatty-acid free BSA (Sigma), pH 7.4). Cellular debris were pelleted at 1000 × *g* for 10 min at 4°C. Supernatants were transferred to new tubes and centrifuged at 3000 × *g* for 10 min at 4°C. Pelleted mitochondria were washed in 5 ml STE + BSA buffer and centrifuged once more at 3000 × *g* for 10 min at 4°C. Pelleted mitochondria were then resuspended in 5 ml STE buffer (250 mM sucrose, 5 mM Tris, 2 mM EGTA, pH 7.4). The final mitochondrial pellets were obtained by centrifugation at 7000 × *g* for 10 min at 4°C and were further resuspended in 1 ml STE buffer. Bradford assays were used to assess protein concentration.

Blue native-polyacrylamide gel electrophoresis (BN-PAGE) and in-gel activity assays

BN-PAGE and complex I and complex IV in-gel activity analyses were performed on mitochondrial extracts from third-instar larvae according to (6). BN-PAGE and complex V in-gel activity were performed on mitochondrial extracts from third-instar larvae, as described in (37) with minor modifications. Briefly, 150 μg of frozen mitochondrial extracts, not thawed before, were lysed in 60 μl solubilization buffer (20 mM Tris-HCl pH 7.4, 0.1 mM EDTA, 50 mM NaCl, 10% glycerol, 1% digitonin). After 15 min incubation on ice, mitochondrial lysates were cleared by pelleting the cellular debris through centrifugation at 13 200 × *g* for 5 min at 2°C. A total of 10 μl of each sample was spared as inputs to assess loading. After addition of 5 μl BN-PAGE loading buffer (final concentration: 0.5% (w/v) Coomassie Blue G-250, 50 mM 6-aminocaproic acid, 10 mM Bis-Tris, pH 7.0), supernatants were loaded on BN-PAGE gels (4–10%). Samples migrated 90 min at 200 V using Coomassie Cathode buffer (50 mM Tricine, 15 mM Bis-Tris, 0.02% Coomassie Blue G-250, pH 7.0) and Anode buffer (50 mM Bis-Tris, pH 7.0). Then Coomassie Cathode buffer was substituted with Cathode buffer without Coomassie Blue (50 mM Tricine, 15 mM Bis-Tris, pH 7.0) and run was completed overnight at 75 V. Afterwards, incubation of the gel for 24 h at 37°C in ATPase in-gel activity buffer (75 mM triethanolamine, 5 mM $MgCl_2$, 0.1% Triton X-100, 0.5 mg/ml lead acetate, 1 mM adenosine triphosphate (ATP) added just before the incubation, pH 8.9) was performed.

Enzyme activity of single respiratory chain complexes

Activities of single respiratory chain complexes from isolated mitochondria of third-instar larvae were monitored according to (43). All enzyme activities were expressed relative to the citrate synthase (CS) activity.

Respiratory rate measurements

Respiratory rate analyses were performed on permeabilized third-instar larvae and on dissected thoraces of 6-day-old adults, as described in (6), with the following modifications. Oxygen consumption was determined at 28°C employing an oxygraph chamber (OROBOROS). The respiratory control rate was determined using 1 mM ADP (state 3) or 1 mM

Table 1. Primers used for cloning, qPCR, qRT-PCR and northern blots

List of primers	
cDNA DmLRPPRC2-GFP for colocalization experiments	
LRPPRC2_EcoRI_GFP_Fusion_F	5′-TGTAAAACGGAATTCATGCAGCGAGCACGACTGTTG-3′
LRPPRC2_BamHI_GFP_Fusion_R	5′-CTATGAGGATCCTCTAACGTGGGCGCGCAGG-3′
cDNA DmLRPPRC2-FLAG for immunoprecipitation experiments	
LRPPRC2_EcoRI_F	5′-CCGGCCGGAATTCATGCAGCGAGCACGACTG-3′
LRPPRC2_XbaI_*FLAG*_Fusion_R	5′-GCCGGCCTCTAGACTA*CTTGTCGTCGTCGTCCTTATA GTC*TCTAACGTGGGCGCGCAG-3′
cDNA DmLRPPRC2 for immunoprecipitation experiments	
LRPPRC2_EcoRI_F	5′-CCGGCCGGAATTCATGCAGCGAGCACGACTG-3′
LRPPRC2_XbaI_R	5′-GCCGGCCTCTAGACTATCTAACGTGGGCGCG-3′
Steady-state levels of mt mRNAs and rRNAs (qRT-PCR and Northern blot)	
qRT-PCR probes	
Taqman probes	**Assay ID**
DMMT-ND1	AI70K4C
DMMT-ND2	AI20SFG
DMMT-ND3	AIFASI7
DMMT-ND4L	AI5IORW
DMMT-ND6	AI6RMX4
DMMT-CYTB	AILJJEB
DMMT-COXIII	AI89JAK
LRPPRC2	Dm01829511_g1
LRPPRC1	Dm01817867_g1
RP49	Dm02151827_g1
SYBR Oligonucleotides	
12S_F	5′-GATAACGACGGTATATAAACTGATTACA-3′
12S_R	5′-GAGGAACCTGTTTTTTAATCGA-3′
16S_F	5′-ACCTGGCTTACACCGGTTT-3′
16S_R	5′-GGGTGTAGCCGTTCAAATTT-3′
ND1_F	5′-AGCCAAACCCCCTCTTCTA-3′
ND1_R	5′-TTTTGATTTTGCTGAAGGAGAAT-3′
ND5_F	5′-TCCTTAGAATAGAATCCAGCTA-3′
ND5_R	5′-AACTTCAGCTTGTTTTAACG-3′
COXI_F	5′-CAGGATGAACTGTTTATCCACCTTT-3′
COXI_R	5′-AATCCCTGCTAAATGTAGAGAAAAAATAG-3′
COXIII_F	5′-CAGACTCAATTTATGGATCAACATT-3′
COXIII_R	5′-AAAGTTGTTCCGATTAATACATGAA-3′
ATP6_F	5′-TGGATGAATTAATCATACACAACAT-3′
ATP6_R	5′-AGGTATAAGAATAGCGGGTGTTC-3′
RP49_F	5′-GACGCTTCAAGGGACAGTATCTG-3′
RP49_R	5′-AAACGCGGTTCTGCATGAG-3′
Northern probes	
CYTB_F	5′-CCTTTACGAAATTCCCATCC-3′
CYTB_R	5′-TGAATCCCTCGGAATTTTCTT-3′
COXI_F	5′-AATGGAGCTGGAACAGGATG-3′
COXI_R	5′-TCGAGGTATTCCAGCCAATC-3′
12S_F	5′-TCATTCTAGATACACTTTCCAGTACATC-3′
12S_R	5′-ACTAAATTGGTGCCAGCAGTCGCGGT-3′
16S_F	5′-AAACCAACCTGGCTTACACC-3′
16S_R	5′-TGAAATGTTATTCGTTTTTAAAGGT-3′
Steady-state levels of mt tRNAs (northern blot)	
$tRNA^{Gly}$	5′-AATAGACCTTATGATTGGAAGTCAA-3′
$tRNA^{Met}$	5′-TGGGGTATGAACCCAGTAGC-3′
$tRNA^{Ser}$	5′-CAAAACATATGCTTATTCAAGCTCA-3′
$tRNA^{Thr}$	5′-TTTTTGATTTACAAGACCAATGTTTT-3′
Steady-state levels of mtDNA (quantitative PCR)	
CYTB_F	5′-TTAATCATATTTGTCGAGACGTT-3′
CYTB_R	5′-AATGATGCACCGTTAGCAT-3′
RP49_F	5′-GACGCTTCAAGGGACAGTATCTG-3′
RP49_R	5′-AAACGCGGTTCTGCATGAG-3′

ADP and 0.25 μg/ml oligomycin (pseudo-state 4). Respiration was uncoupled by adding 4 μM CCCP and the complex I contribution to the respiratory chain proton flux was inhibited by adding 6 μM rotenone.

DNA isolation and quantitative polymerase chain reaction (qPCR)

Isolation of total DNA from third-instar larvae and 6-day-old adults was done by using the DNeasy Blood & Tissue kit (Qiagen). To assess mtDNA levels, qPCR experiments were carried out with a 7900HT Fast Real-Time PCR System (Applied Biosystems). Each sample was present in duplicate and contained ∼5 ng total DNA, 10 μM specific SYBR primers and the Platinum SYBR Green qPCR SuperMix-UDG with ROX (Invitrogen) in a 12 μl volume. Levels of mtDNA were determined by using primers for the *cytb* gene and normalized to levels of the ribosomal protein 49 gene (*rp49*). The SYBR primers are listed in Table 1.

RNA isolation, quantitative reverse transcription-PCR (qRT-PCR) and northern blot analysis

Isolation of total RNA from third-instar larvae and 6-day-old adults was performed using the ToTALLY RNA Total RNA isolation kit (Ambion). For qRT-PCR experiments, DNase treatment was performed using the TURBO DNA-free^{TM} kit (Ambion). Reverse transcription was carried out with the High capacity cDNA Reverse Transcription kit (Applied Biosystem). For RNA quantification, qRT-PCR experiments were performed with a 7900HT Fast Real-Time PCR System (Applied Biosystems). Each sample was analyzed in duplicate and contained ∼25 ng total RNA. Cytoplasmic *rp49* RNA was used as a reference. TaqMan probes and SYBR primers are listed in Table 1.

For northern blot experiments, 2 μg of total extracted RNA was denatured for 20 min at 65°C after addition of NorthernMax-Gly Sample Loading Dye (Ambion). The RNA samples were electrophoresed in 1.2% agarose gels containing MOPS/formaldehyde. Next, the separated RNA was transferred to Hybond-N+ nylon membranes (GE Healthcare). Different mRNAs and rRNAs were detected after hybridization with α-^{32}P-dCTP-labeled DNA probes, obtained by using the Prime-It II random primer labeling kit (Stratagene). Different tRNAs were detected after hybridization with γ-^{32}P-ATP-labeled tRNA oligonucleotides. Radioactivity was detected by exposure to PhosphoImager Screens and X-ray films, and quantification was performed using Molecular Imager FX (Bio-Rad). Cytosolic *rp49* RNA levels were used as a reference. DNA probes and oligonucleotides are listed in Table 1.

In organello de novo transcription and translation assays

In organello (*de novo*) transcription and translation assays were performed as described in (6). Concerning *in organello* translation pulse and chase experiments, after pulse the isolated mitochondria, previously treated with translation buffer (100 mM Mannitol, 10 mM Sodium succinate, 80 mM KCl, 5 mM $MgCl_2$, 1 mM KH_2PO_4, 25 mM Hepes pH 7.4, 60 μg/ml all amino acids except Met, 5 mM ATP, 0.2 mM GTP, 6 mM creatine phosphate, 60 μg/ml creatine kinase) supplemented with ^{35}S-Met, were washed four times with translation buffer before chase to ensure appropriate removal of ^{35}S-Met residues.

Ribosomal and RNA analyses using sucrose density gradient assay

Mitochondrial extracts from third-instar larvae were obtained as previously described. The final mitochondrial pellets were washed four times in EDTA buffer (154 mM KCl, 5 mM MOPS, 1 mM EDTA, pH 7.4) to ensure removal of cytoplasmic ribosomes according to (44). Bradford assays were used to assess protein concentrations.

Sucrose density ultracentrifugation of ribosome components was carried out as described previously (7,45), with the following modifications. Isolated mitochondria (3–4 mg) were incubated on ice for 20 min in lysis buffer (260 mM sucrose, 100 mM NH_4Cl, 10 mM $MgCl_2$, 30 mM Tris-HCl pH 7.5, 40 U/ml RNase Inhibitor Human Placenta (NEB), 1% Triton X-100) supplemented with EDTA-free complete protease inhibitor cocktail (Roche) and PhosSTOP phosphatase inhibitor cocktail (Roche). Mitochondrial lysates were cleared by pelleting the cellular debris through centrifugation at 9200 × *g* for 45 min at 4°C. Supernatants were gently loaded on the top of 10–34% linear sucrose gradients made in a buffer containing 100 mM NH_4Cl, 10 mM $MgCl_2$, 30 mM Tris-HCl pH 7.5 and EDTA-free complete protease inhibitor cocktail (Roche). Afterwards, samples were centrifuged at 1.16 × 10^5 *g* for 16 h at 4°C and fractions (∼500 μl each) from the sucrose gradient sedimentation were collected using a Teledyne density gradient fractionator. The ribosomal profiles were obtained by continuous monitoring at 252 nm absorbance. For rRNA and mRNA sedimentation profile analyses, RNA was extracted from each fraction using TRIzol LS Reagent (Invitrogen) according to the manufacturer's recommendations. Afterwards, RNA was DNase-treated, reverse transcribed and quantified through absolute qRT-PCR analyses. All analyses were performed as previously described. For the detection of mitochondrial transcripts, qRT-PCR was performed in reactions using either a Taqman probe or SYBR primers, as previously described. Each fraction was analyzed in duplicate and the average value of each duplicate was used to determine RNA expression levels through the 2-ΔΔCt method. From each sample, the RNA quantity in each fraction was calculated as percentage relative to the sum of RNA abundance from all fractions. The used Taqman probes and SYBR primers correspond to those ones listed in Table 1.

Generation of transgenic lines overexpressing DmLRPPRC2 with or without a FLAG tag

The full-length *Drosophila melanogaster Lrpprc2* cDNA sequence was obtained from the UT01249 clone (DGC, BDGP). The previously described non-synonymous nucleotide substitutions were corrected and the sequence was cloned into the pUASTattB vector. For the generation of the *Flag*-tagged *DmLrpprc2* clone, a *Flag* tag was added to the C-terminus of the *DmLrpprc2* sequence. For the generation

of the transgenic flies, both pUASTattB plasmids containing either *DmLrpprc2* or *DmLrpprc2-Flag* constructs were injected in *Drosophila* embryos carrying attP40 insertion sites. The primers employed for cloning are listed in Table 1.

FLAG-protein immunoprecipitation

Mitochondrial extracts from third-instar larvae overexpressing FLAG-tagged DmLRPPRC2 (w;UAS-*Lrpprc2-Flag*/+;*da*GAL4/+), or overexpressing wild-type DmLRPPRC2 (w;UAS-*Lrpprc2*/+;*da*GAL4/+) were obtained as previously described. The samples obtained from larvae expressing DmLRPPRC2 without FLAG tag were considered as control for the binding activity of the DmLRPPRC2-FLAG protein. FLAG-protein immunoprecipitation assays, SDS-PAGE, staining and mass spectrometry analyses were performed. Briefly, 1–2 mg of mitochondria suspension was pelleted by centrifugation at 12 000 × *g* for 5 min at 4°C. Pelleted mitochondria were resuspended in 1 ml lysis buffer (50 mM Tris-HCl pH 7.4, 150 mM NaCl, 1 mM EDTA, 3% Glycerol, 0.5% Triton X-100) supplemented with EDTA-free complete protease inhibitor cocktail (Roche) and PhosSTOP phosphatase inhibitor cocktail (Roche). After 20 min incubation on ice, lysis was completed by 10 times passage through a 27G needle. Mitochondrial lysates were cleared by pelleting the cellular debris through centrifugation at 14 000 × *g* for 10 min at 4°C. A total of 20 μl aliquots of supernatants was kept as inputs. In the meanwhile a FLAG M2 resin suspension (Roche) was washed four times in 1 ml lysis buffer. Supernatants were incubated with 50 μl FLAG M2 resin suspension (Roche) for 2–3 h at 4°C on a rotating wheel. Afterwards the resin was pelleted by centrifugation at 3000 × *g* for 1 min at 4°C and the supernatants were collected as flow-through (F.T.). The resin was washed five times with the lysis buffer. For the elution, beads were incubated on ice in 100 μl reversion buffer (100 mM Glycine, pH 2.5) and supernatants were collected after centrifugation at 3000 × *g* for 1 min at 4°C. pH was adjusted by adding 2 μl 1 M Tris. Eluates were evaporated under speed vacuum for 20 min at 45°C until the volume reached 40 μl. Note that Laemmli buffer (final concentration: 1% SDS, 5% Glycerol, 30 mM Tris, 0.005% Bromophenol Blue, 350 mM 2-Mercaptoethanol) was added and samples were split: three-fourth for mass-spectrometry and one-fourth for western blot experiments. For mass spectrometry analyses, samples were denatured at 95°C for 5 min followed by SDS-PAGE on 4–20% Criterion Tris-HCl precast SDS-PAGE gels (Bio-Rad). The gels were silver stained through the SilverQuest™ Silver Staining (Invitrogen) or Coomassie stained through the Roti®-Blue quick solution (Roth). For mass spectrometry analyses, the number of peptides and coverage were calculated from values obtained using the Uniprot KB database. Western blot experiments were performed as previously described using 4–20% Criterion Tris-HCl pre-cast SDS-PAGE gels (Bio-Rad). DmLRPPRC2 and DmLRPPRC2-FLAG protein expression in inputs, F.T. and eluate fractions was determined by using the following primary antibodies: FLAG M2 (Sigma, dilution 1:500) and a polyclonal rabbit antiserum raised against DmLRPPRC2 (generated by PSL GmbH, dilution 1:1000).

Statistical analyses

Data are reported as mean ± 1 SD or mean ± SEM. For statistical analyses, Mann–Whitney test was used to analyze the climbing index, the log-rank test was used to analyze lifespan and the unpaired *t*-test was used to analyze all other data.

RESULTS

DmLRPPRC2 is a mitochondrial protein

The DmLRPPRC2 protein is the *Drosophila* co-ortholog to mammalian LRPPRC and it has lower protein sequence identity and similarity to HsLRPPRC than DmLRPPRC1 (Supplementary Figure S1A). *In silico* analysis identified the presence of 22 PPR motifs distributed throughout the DmLRPPRC2 protein. Interestingly, the distribution of PPR motifs in DmLRPPRC2 is very similar to the distribution of PPR motifs in DmLRPPRC1 and HsLRPPRC (Supplementary Figure S1A). However, the additional carboxy-terminal segment observed in the DmLRPPRC1 and HsLRPPRC proteins suggests a functional difference between the DmLRPPRC1 and DmLRPPRC2 paralogs (Supplementary Figure S1A and B).

Bioinformatic predictions from two different databases suggest that DmLRPPRC2 is a mitochondrial protein (MitoProtII probability for mitochondrial localization 99.7% and TargetP 1.1 probability 95.7%), consistent with previous reports that PPR domain proteins are mainly targeted to mitochondria or chloroplasts (8,9). An N-terminal mitochondrial targeting peptide of 70 amino acids is predicted by TargetP 1.1 (Supplementary Figure S1B). To verify the validity of these predictions we determined the subcellular localization of DmLRPPRC2 by fluorescence confocal microscopy of HeLa cells transfected with a DmLRPPRC2-AcGFP1 fusion construct. There was a very high co-localization rate (96.4 ± 2.6%) between the DmLRPPRC2-AcGFP1 fluorescence and the mitochondrial network stained with the MitroTracker Deep Red dye (Figure 1A). In addition, we performed subcellular fractionation experiments in flies that showed that the DmLRPPRC2 protein is present in the mitochondrial fraction (Figure 1B). The results from bioinformatic predictions, fluorescence microscopy and subcellular fractionation are thus consistent with a predominant mitochondrial localization of DmLRPPRC2.

Efficient suppression of *DmLrpprc2* gene expression by RNA interference (RNAi)

To investigate DmLRPPRC2 protein function in mitochondria, we downregulated the expression of the *DmLrpprc2* gene by utilizing RNAi mediated by the UAS-GAL4 binary system (46) (Figure 2A–D). We used two independent transgenic RNAi lines that target different and non-overlapping sequences of the *DmLrpprc2* mRNA. Ubiquitous RNAi expression was achieved by crossing the constitutive *daughterless*-GAL4 (*da*GAL4) driver line with either of the two *DmLrpprc2* RNAi lines, thereby generating two different KD lines: w;UAS-*Lrpprc2*RNAi#1/+;*da*GAL4/+ and w;;UAS-*Lrpprc2*RNAi#2/*da*GAL4 (henceforth denoted *Lrpprc2*RNAi#1 and *Lrpprc2*RNAi#2, respectively).

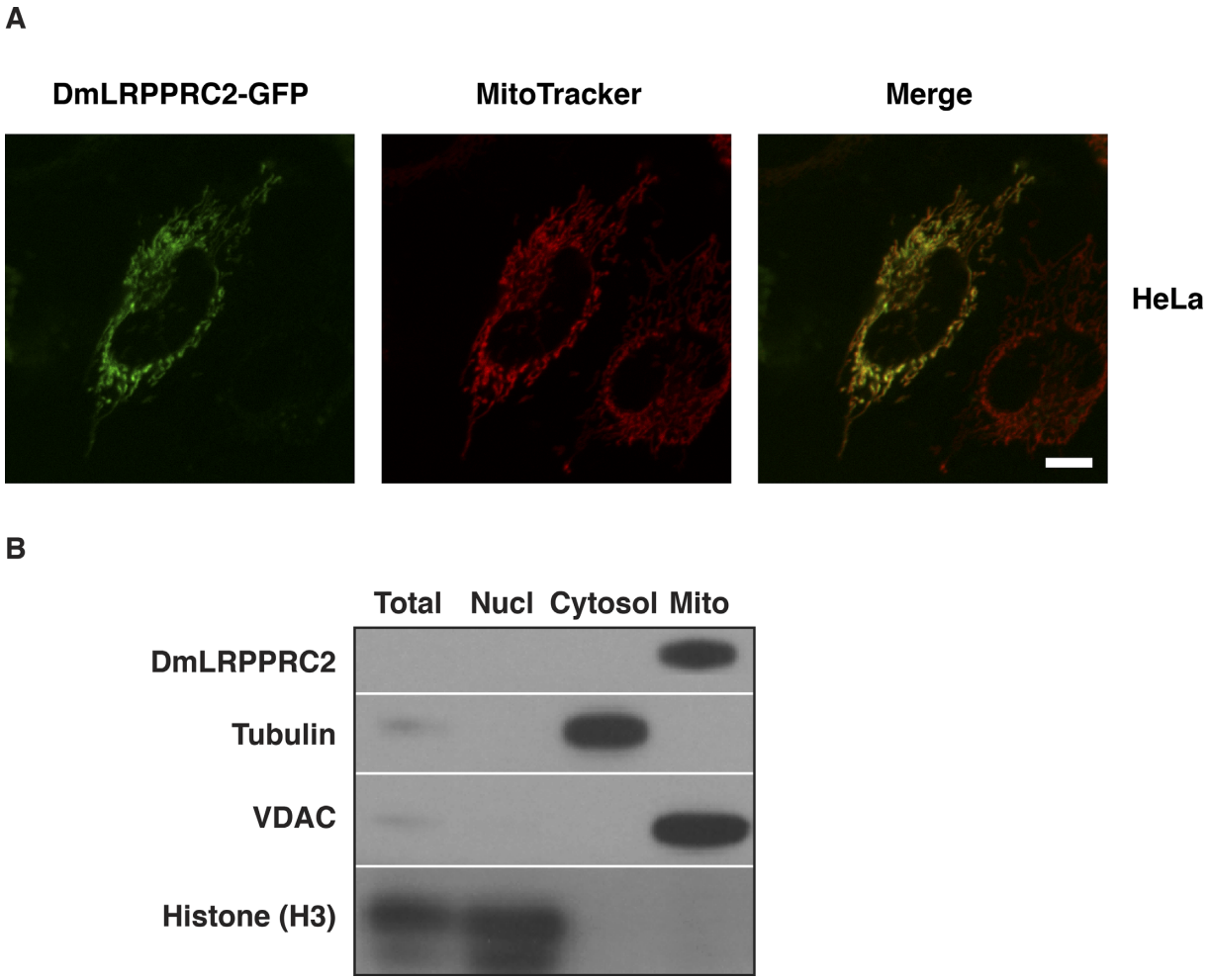

Figure 1. Subcellular localization of DmLRPPRC2. (A) Fluorescence confocal microscopy images showing HeLa cells ($n = 15$) expressing a DmLRPPRC2-GFP fusion protein and counterstained with the mitochondrial marker MitoTracker Deep Red. Scale bar: 10 μm. (B) Subcellular fractionation showing the presence of DmLRPPRC2 in the mitochondrial fraction. Subcellular fractions were separated by SDS-PAGE followed by western blot analysis to detect histone H3 (a nuclear marker), tubulin (a cytosolic marker), VDAC (a mitochondrial marker) and DmLRPPRC2. See also Supplementary Figure S1A and B.

The lines used as controls were: w;;*da*GAL4/+, w;UAS-*Lrpprc2*RNAi#1/+ and w;;UAS-*Lrpprc2*RNAi#2/+.

We assessed the expression of the *DmLrpprc2* gene by qRT-PCR experiments. Upon constitutive RNAi expression, *DmLrpprc2* transcript levels were efficiently downregulated in third-instar larvae in both the *Lrpprc2*RNAi#1 line (∼70% reduction; Figure 2A) and the *Lrpprc2*RNAi#2 line (∼80% reduction; Figure 2C). The downregulation of *DmLrpprc2* gene expression in larvae was thus very prominent and persisted into adulthood albeit with somewhat reduced efficiency (∼50% reduction in both *DmLrpprc2* KD lines; Figure 2A and C). Western blot analyses performed on isolated mitochondria from third-instar larvae showed an almost complete absence of DmLRPPRC2 protein in both *DmLrpprc2* KD lines (Figure 2B and D), confirming efficient downregulation of *DmLrpprc2* expression.

To assess specificity of the *Lrpprc2*RNAi#1 and *Lrpprc2*RNAi#2 lines, we measured *DmLrpprc1* mRNA levels. We found ∼2-fold increase of *DmLrpprc1* transcript levels at the third-instar larval stage in both *DmLrpprc2* KD lines, whereas only a slight increase was observed at the adult stage (Figure 2A and C). Western blot experiments performed on isolated mitochondria from third-instar larvae of both *DmLrpprc2* KD lines showed increased steady-state levels of DmLRPPRC1 protein (Figure 2B and D). These findings show that both RNAi lines specifically target the *DmLrpprc2* transcript, despite the fact that there is substantial nucleotide sequence homology (57% sequence identity) between the *DmLrpprc1* and *DmLrpprc2* transcripts. Interestingly, DmLRPPRC2 protein levels were increased in mitochondria isolated from *DmLrpprc1* KD third-instar larvae (Supplementary Figure S2). This reciprocal expression, i.e. the finding that the expression of *DmLrpprc1* increases when *DmLrpprc2* is downregulated and *vice versa*, might be explained by gene-specific regulatory mechanisms or by a general induction of compensatory mitochondrial biogenesis.

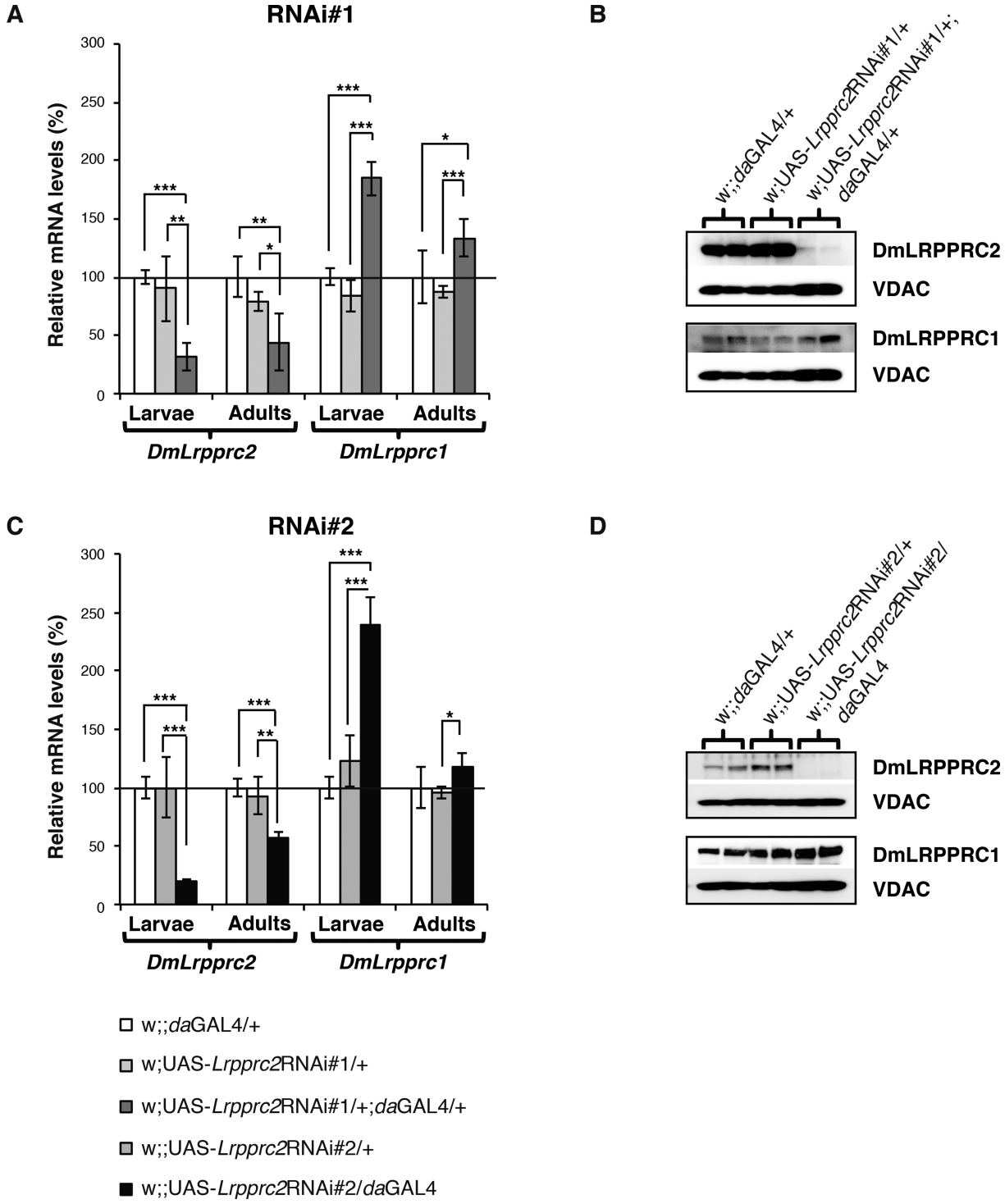

Figure 2. Efficient ubiquitous downregulation of *DmLrpprc2* expression. (A) qRT-PCR analyses of *DmLrpprc2* and *DmLrpprc1* mRNA levels in the *Lrpprc2*RNAi#1 line measured in controls (white and light gray bars) and *DmLrpprc2* KD (dark gray bars) third-instar larvae and 6-day-old flies ($n = 4$–5). Error bars indicate mean ± 1 SD. Student's *t*-test was applied, $^{*}P < 0.05$, $^{**}P < 0.01$, $^{***}P < 0.001$. (B) Western blot experiments to detect DmLRPPRC2 and DmLRPPRC1 in the *Lrpprc2*RNAi#1 line. Mitochondrial protein extracts (40 μg) from control and *DmLrpprc2* KD third-instar larvae were separated by standard SDS-PAGE, followed by western blot analysis with antibodies against DmLRPPRC2, DmLRPPRC1 and VDAC, the latter used as reference for loading. (C) qRT-PCR analyses of *DmLrpprc2* and *DmLrpprc1* mRNA levels in the *Lrpprc2*RNAi#2 line measured in controls (white and light gray bars) and *DmLrpprc2* KD (black bars) third-instar larvae and 6-day-old flies ($n = 4$–5). Error bars indicate mean ± 1 SD. Student's *t*-test was applied, $^{*}P < 0.05$, $^{**}P < 0.01$, $^{***}P < 0.001$. (D) Western blot experiments to detect DmLRPPRC2 and DmLRPPRC1 in the *Lrpprc2*RNAi#2 line. Mitochondrial protein extracts (40 μg) from control and *DmLrpprc2* KD third-instar larvae were separated by standard SDS-PAGE, followed by western blot analysis with antibodies against DmLRPPRC2, DmLRPPRC1 and VDAC, the latter used as reference for loading. See also Supplementary Figure S2.

Ubiquitous downregulation of *DmLrpprc2* gene expression affects development, climbing ability and lifespan

Ubiquitous suppression of *DmLrpprc2* gene expression caused developmental delay with a severe reduction in body size at the 6-day-old larval stage (Figure 3A), and reduced eclosion rates (Figure 3B). Interestingly, only ∼15% of the pupae eclosed from the *Lrpprc2*RNAi#1 line, whereas most of the pupae, ∼75%, eclosed from *Lrpprc2*RNAi#2 line (Figure 3B). The high eclosion rate in the *Lrpprc2*RNAi#2 line allowed us to further quantify the locomotor and negative geotaxis behavior in adults through climbing tests. At age 13 days, the *DmLrpprc2* KD males showed a significantly reduced climbing ability, suggesting a neuromuscular impairment (Figure 3C). Additionally, the lifespan of both *DmLrpprc2* KD lines was significantly shortened with an average lifespan of 42 and 55 days, respectively, and a maximal lifespan of 60 and 70 days, respectively (Figure 3D). In contrast, the controls had an average lifespan of 70–75 days and a maximal lifespan of 95–105 days (Figure 3D).

DmLrpprc2 KD causes severe respiratory chain dysfunction

The phenotypical abnormalities observed upon *DmLrpprc2* KD (delayed development, impaired climbing skills and reduced survival) and the mitochondrial localization of the DmLRPPRC2 protein prompted us to investigate the mitochondrial respiratory chain activity. Western blot analysis showed that the steady-state levels of the NDUFS3 subunit of the complex I was reduced at the larval and adult stages in both KD lines (Figure 4A). In contrast, the steady-state levels of the α-subunit of ATP synthase (complex V) remained unchanged in both KD lines (Figure 4A). The levels of assembled complex I and IV and the corresponding in-gel enzyme activities were reduced on BN-PAGE at the larval stage in both KD lines (Figure 4B). In addition, complex V (ATP synthase) oligomerization status and in-gel activity on BN-PAGE were markedly affected at the larval stage in both KD lines, showing accumulation of subassemblies (*sub*CV_a and *sub*CV_b; Figure 4B). We proceeded to measure respiratory chain enzyme activities and found a significant reduction of the activities of complex I, complex I–III and complex IV in mitochondria from third-instar larvae from the *Lrpprc2*RNAi#2 line (Figure 5A). In contrast, the complex II activity, exclusively dependent on nuclear-encoded subunits, and the complex II–III activity were increased in the *Lrpprc2*RNAi#2 line (Figure 5A). To assess oxidative phosphorylation in intact mitochondria, we measured the oxygen consumption rate in permeabilized larvae and fly thoraces (Figure 5B). Interestingly, we found that the uncoupled oxygen consumption rate assessed in the presence of substrates that deliver electrons to the respiratory chain at the level of complex I (CPI; pyruvate, glutamate, malate, proline) was decreased by 50% in third-instar KD larvae and by 80% in thoraces of adult KD flies (Figure 5B). Furthermore, addition of a combination of substrates delivering electrons at the levels of complex I, complex II and glycerol-3-phosphate dehydrogenase (CPI-SUCC-G3P; pyruvate, glutamate, malate, proline, succinate and glycerol-3-phosphate) revealed that the uncoupled oxygen consumption rate was decreased in thoraces of adult KD flies (Figure 5B). Based on these results we conclude that depletion of DmLRPPRC2 leads to deficient oxidative phosphorylation, which, in turn, is a likely cause of the observed phenotypic manifestations in KD larvae and flies.

DmLRPPRC2 does not control mitochondrial transcript stability

Loss of DmLRPPRC2 causes a severe reduction in the activities of complexes I, IV and V, which all contain critical mtDNA-encoded subunits, whereas the activity of complex II, which is solely dependent on nucleus-encoded subunits, is normal. This type of respiratory chain deficiency is typically seen if there is a global reduction in mtDNA expression (5,45,47) and we therefore proceeded with a detailed characterization of the underlying molecular cause.

First, we focused on mitochondrial transcription and found normal steady-state levels of most mitochondrial mRNAs by qRT-PCR and northern blot analyses of *DmLrpprc2* KD larvae and adult flies (Figure 6A–E). The *coxIII* mRNA was moderately increased in both larvae and adults, whereas the *nd1* and *nd2* mRNAs were moderately decreased at the adult stage (Figure 6A). The levels of the *12S* and *16S* rRNAs were normal in *DmLrpprc2* KD larvae, whereas the levels were normal or increased in adult KD flies (Figure 6B–E, Supplementary Figure S3). The levels of the analyzed tRNAs were normal or increased in *DmLrpprc2* KD larvae and generally increased in adult KD flies (Figure 6B–E).

The finding of normal levels of most analyzed mRNAs in *DmLrpprc2* KD larvae and flies is in sharp contrast to the profound reduction in levels of most mRNAs in *DmLrpprc1* KD flies (6). These results show that DmLRPPRC2 has no major influence on the stability of mitochondrial mRNAs and that reduced mRNA levels do not explain the observed global decrease in respiratory chain function.

DmLrpprc2 KD increases mitochondrial *de novo* transcription

The observed increase in steady-state levels of tRNAs upon *DmLrpprc2* KD (Figure 6B–E) prompted us to investigate mitochondrial *de novo* transcription. We performed *in organello* labeling experiments in isolated mitochondria from third-instar larvae and found a strong general increase of transcription in *DmLrpprc2* KDs at the larval stage (Figure 7A). These findings are in good agreement with our previous observations that increased steady-state levels of tRNAs correlate well with an increase of mitochondrial *de novo* transcription (5,6,45,47). The increase of *de novo* transcription cannot be explained by more templates as the mtDNA steady-state levels were only mildly increased in *DmLrpprc2* KD larvae, whereas no significant changes were observed in *DmLrpprc2* KD adults (Figure 7B). The increased synthesis of mitochondrial RNAs may represent a compensatory response triggered by the mitochondrial respiratory chain dysfunction.

DmLRPPRC2 does not control mitochondrial transcript polyadenylation

We have previously reported that *DmLrpprc1* and *Lrpprc* are essential for polyadenylation of mtDNA-encoded

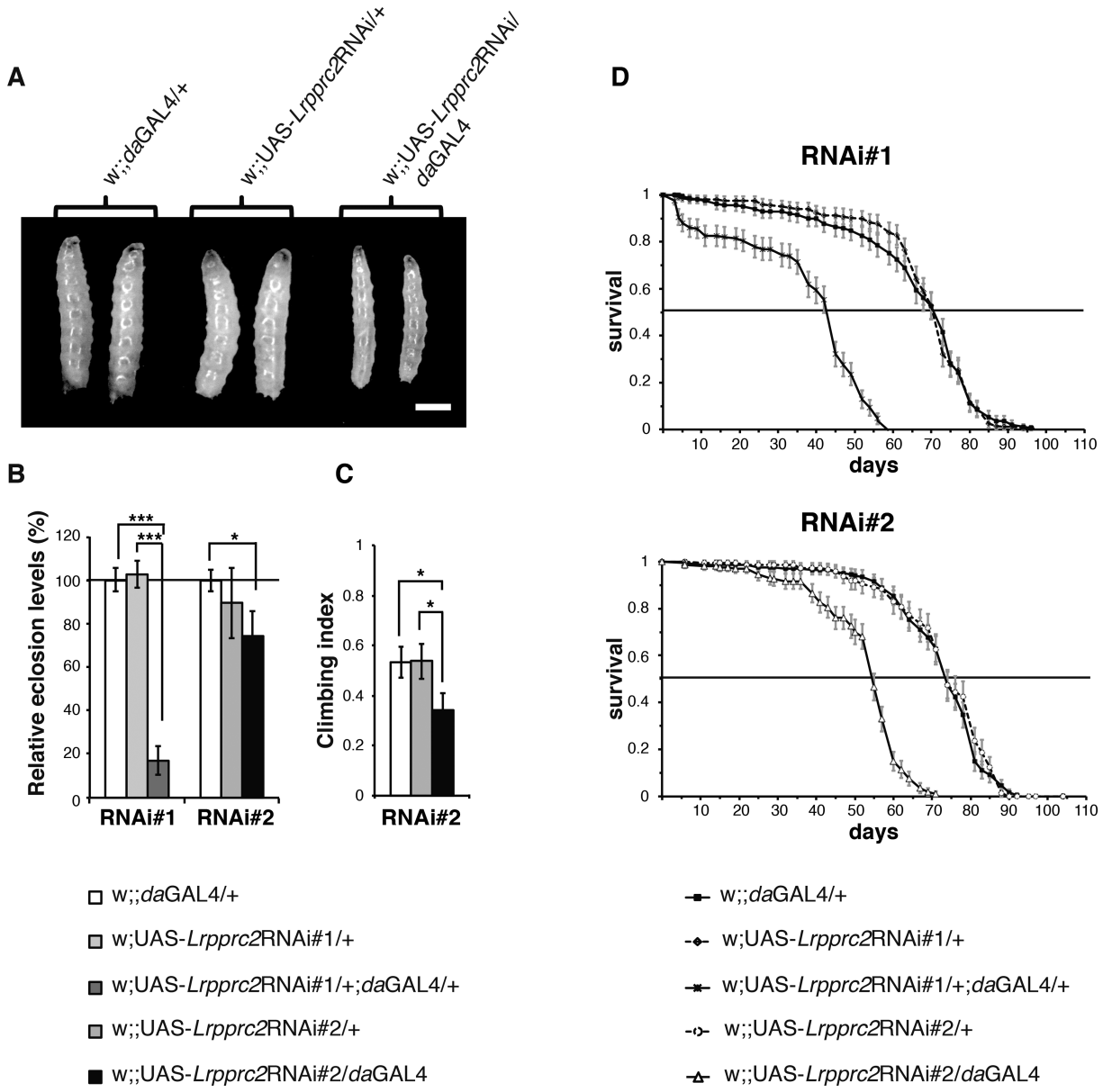

Figure 3. Larval size, eclosion, climbing index and lifespan analyses. (A) Body size comparison at the 6-day-old third-instar larval stage showing reduced size for *DmLrpprc2* KD larvae compared to controls. Scale bar: 1 mm. (B) Eclosion rates of the *Lrpprc2*RNAi#1 line (left) and the *Lrpprc2*RNAi#2 line (right) in control (white and light gray bars) and *DmLrpprc2* KD (dark gray and black bars) individuals. Data are shown relative to the w;;*da*GAL4/+ control line. Error bars indicate mean ± 1 SD. Student's *t*-test was applied, $^{*}P < 0.05$, $^{**}P < 0.01$, $^{***}P < 0.001$. (C) Climbing test on males of the *Lrpprc2*RNAi#2 line, showing impaired climbing skills of 13-day-old *DmLrpprc2* KD individuals ($n = 12$) in comparison to controls ($n = 5$–6). Error bars indicate mean ± 1 SD. Mann–Whitney U test was applied, $^{*}P < 0.05$. (D) Survival curves of the *Lrpprc2*RNAi#1 line (upper graph) and the *Lrpprc2*RNAi#2 line (lower graph), showing shortened lifespan for *DmLrpprc2* KD individuals in comparison to controls. Error bars indicate mean ± 1 SD. Long-rank test was applied.

mRNAs in flies and mice, respectively (6,7). We therefore investigated whether defective polyadenylation could explain the profound respiratory chain deficiency observed in *DmLrpprc2* KD flies. To this end, we circularized and reverse transcribed RNAs extracted from isolated mitochondria of third-instar larvae. Sequencing of the 3′ ends of 8 mitochondrial transcripts (*nd1*, *nd4*, *nd5*, *nd6*, *cytb*, *coxI*, *coxII*, *atp8/6*) showed no evident reduction in the polyA tail length in *DmLrpprc2* KD larvae (Supplementary Figure S4). These analyses included the *cytb* and *atp8/6* mRNAs, which were the only mRNAs showing normal polyadenylation profiles in *DmLrpprc1* KD flies (6). Based on these findings we conclude that the essential role for DmLRPPRC2 in regulation of mtDNA expression does not involve the control of mRNA stability or polyadenylation. These findings show that DmLRPPRC2 is a novel regulator of mitochondrial gene expression with an independent mode of action in comparison to its paralog DmLRPPRC1.

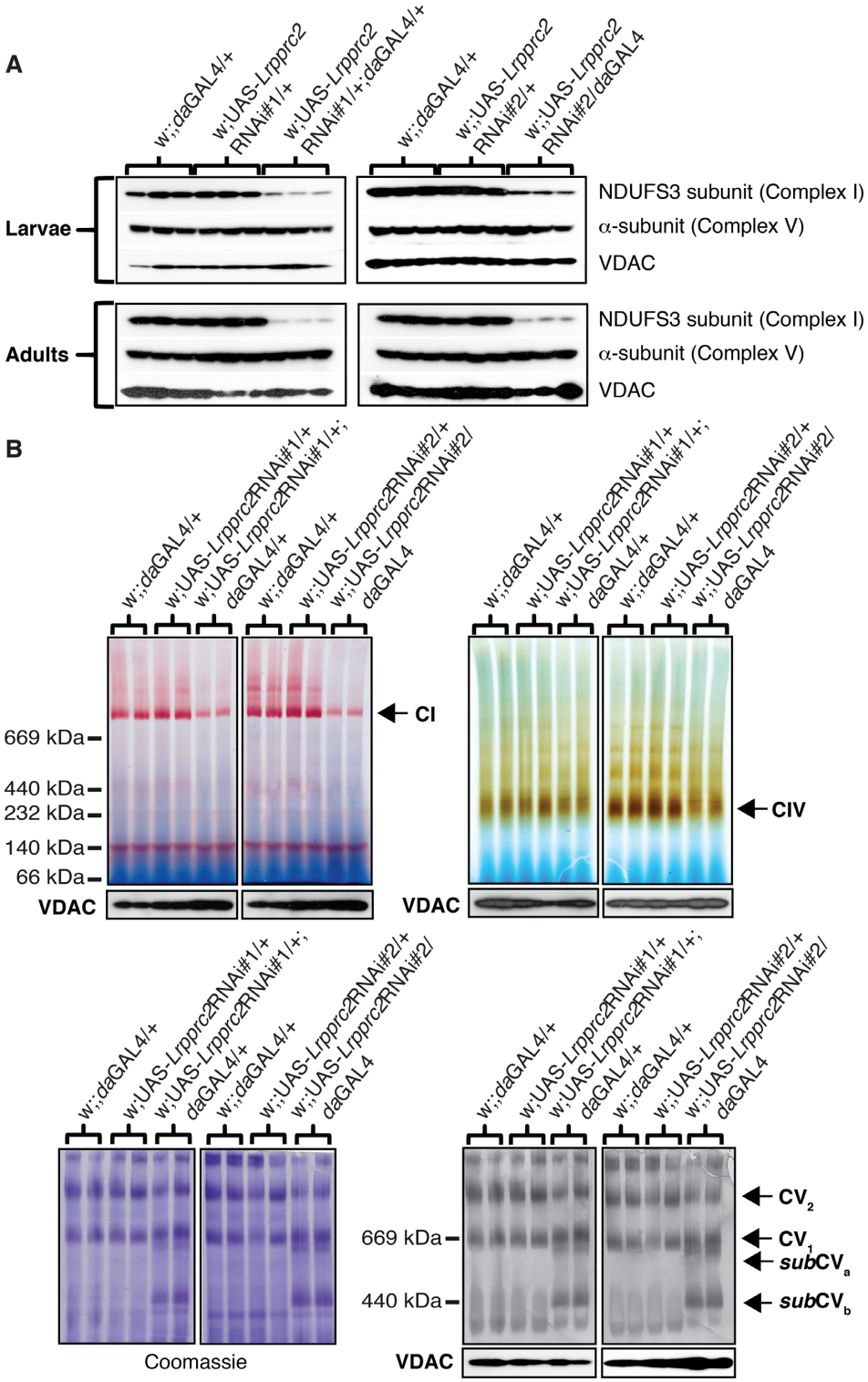

Figure 4. Steady-state levels and activities of the OXPHOS complexes. (A) Western blot analysis of the *Lrpprc2*RNAi#1 line (left side) and the *Lrpprc2*RNAi#2 line (right side) performed on 20–40 μg whole-body protein extracts from controls and *DmLrpprc2* KD third-instar larvae and 6-day-old adults. Protein extracts were separated by standard SDS-PAGE followed by western blot analysis with antibodies against the nuclear-encoded subunit NDUFS3 of complex I, the α-subunit of complex V and VDAC, the latter used as reference for loading. (B) BN-PAGE combined with complex I, complex IV and complex V in-gel activity analyses on the *Lrpprc2*RNAi#1 line and the *Lrpprc2*RNAi#2 line. BN-PAGE was performed on 75 μg for complex I, 100 μg for complex IV and 150 μg for complex V of mitochondrial protein extracts from control and *DmLrpprc2* KD third-instar larvae. The assembly status of complex V (right panel) is black because of color inversion. Loading controls are provided by Coomassie staining to assess the total mitochondrial protein content per sample (only for complex V, left panel) and western blot analysis of VDAC protein levels in mitochondrial protein lysates collected prior to BN-PAGE gel loading. The position of complex I (CI), complex IV (CIV), complex V dimers (CV_2), complex V monomers (CV_1) and complex V subassembled components (*sub*CV_a and *sub*CV_b) are indicated by arrows.

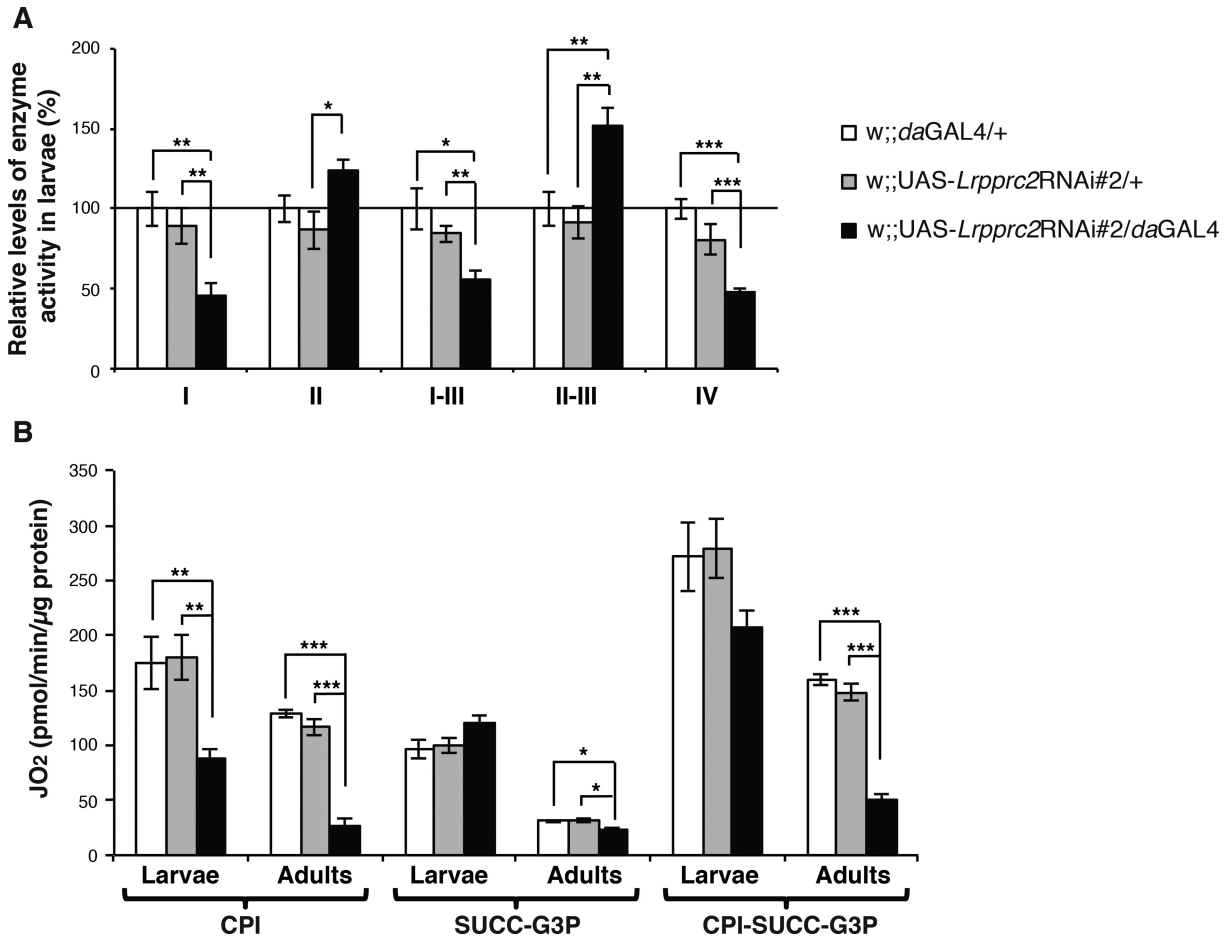

Figure 5. Biochemical measurement of respiratory chain function. (A) Respiratory chain enzyme activities, normalized to the CS activity, were used to assess the activities of complex I (NADH coenzyme Q reductase, reported as I), complex II (succinate dehydrogenase, reported as II), complexes I–III (NADH coenzyme Q reductase-cytochrome c reductase, reported as I–III), complexes II–III (succinate dehydrogenase-cytochrome c reductase, reported as II–III) and complex IV (cytochrome c oxidase, reported as IV) in isolated mitochondria from control (white and gray bars) and *DmLrpprc2* KD (black bars) third-instar larvae of the *Lrpprc2*RNAi#2 line ($n = 6$–12). Error bars indicate mean ± SEM. Student's *t*-test was applied, $^{*}P < 0.05$, $^{**}P < 0.01$, $^{***}P < 0.001$. (B) Oxygen consumption measurements normalized to protein content in permeabilized control (white and gray bars) and *DmLrpprc2* KD (black bars) third-instar larvae and thoraces from 6-day-old adults of the *Lrpprc2*RNAi#2 line ($n = 5$). Respiratory rate analyses were performed using substrates delivering electrons at the level of complex I (CPI), complex II and glycerol-3-phosphate dehydrogenase (SUCC-G3P), or by using combined substrates delivering electrons at the level of complex I, II and glycerol-3-phosphate dehydrogenase (CPI-SUCC-G3P). Error bars indicate mean ± SEM. Student's *t*-test was applied, $^{*}P < 0.05$, $^{**}P < 0.01$, $^{***}P < 0.001$.

DmLRPPRC2 coordinates mitochondrial translation

To elucidate further how mitochondrial gene expression is affected when DmLRPPRC2 is depleted, we investigated mitochondrial *de novo* protein synthesis. We performed *in organello* labeling experiments in mitochondria extracted from third-instar larvae and found an increase of several *de novo* synthesized mitochondrial proteins and a concomitant decrease of other translation products, without any presence of apparently truncated translation products (Figure 7C). A particularly strong increased synthesis was observed for ND1, ND3, ND4L, CYTB, ATP6 and ATP8, whereas the synthesis of COXI, ND4 and ND2 was severely reduced. The synthesis of ND6, COXII and COXIII was unaffected or only mildly increased in *DmLrpprc2* KD mitochondria (Figure 7C). We checked whether the newly synthesized proteins were subjected to enhanced degradation by performing chase with cold methionine at two different time-points (3 and 5 h) and found that they remained equally stable in control and *DmLrpprc2* KD mitochondria (Figure 7C).

The dramatic increment of some newly synthesized mitochondrial proteins and the severe decrease of other ones prompted us to perform more detailed analyses to determine how DmLRPPRC2 influences mitochondrial translation. We performed sucrose density gradient experiments on mitochondrial preparations from control and *DmLrpprc2* KD third-instar larvae. These experiments were based on ultracentrifugation of mitochondrial lysates at the top of a 10–34% sucrose gradient and on subsequent collection of 20 fractions from the bottom to the top of the gradient. qRT-PCR analyses were performed to quantify the distribution of single mitochondrial transcripts in relation to the mitochondrial small (28S) and large (39S) ribosomal subunits and the fully assembled (55S) ribosome (Figure 8 and Supplementary Figure S5). In control samples, all of the

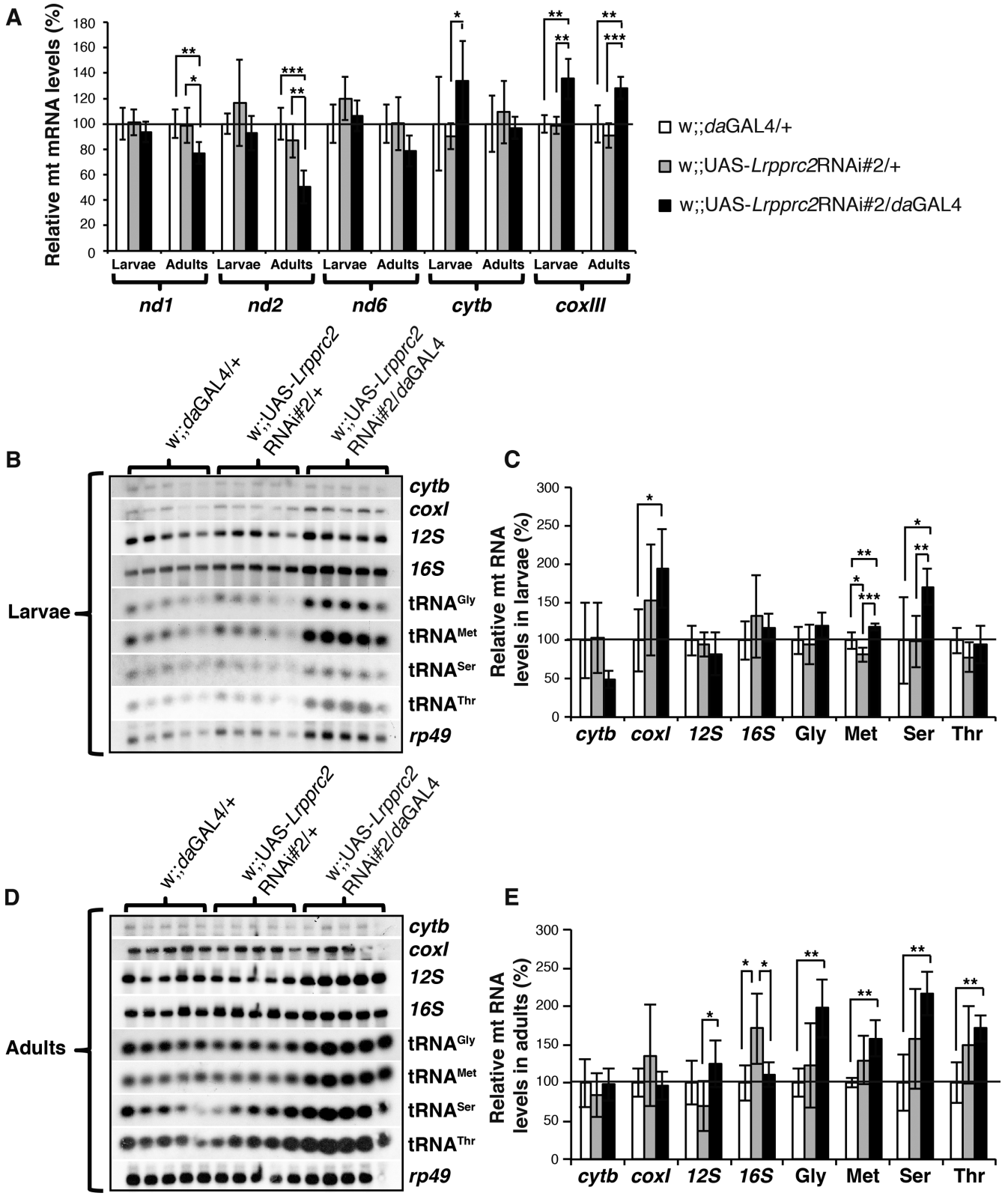

Figure 6. Steady-state levels of mitochondrial mRNAs, rRNAs and tRNAs. (A) qRT-PCR analyses on mitochondrial mRNAs normalized to the nuclear ribosomal protein 49 (*rp49*) transcript levels in control (white and gray bars) and *DmLrpprc2* KD (black bars) third-instar larvae or 6-day-old adults of the *Lrpprc2*RNAi#2 line ($n = 4$–5). Error bars indicate mean ± 1 SD. Student's *t*-test was applied, $^{*}P < 0.05$, $^{**}P < 0.01$, $^{***}P < 0.001$. (B) Northern blot analyses of steady-state levels of mitochondrial mRNAs, rRNAs and tRNAs, normalized to the *rp49* transcript levels, in third-instar larvae of the *Lrpprc2*RNAi#2 line. (C) Quantification of northern blots shown in panel B. Error bars indicate mean ± 1 SD. Student's t-test was applied, $^{*}P < 0.05$, $^{**}P < 0.01$, $^{***}P < 0.001$. (D) Northern blot analyses of steady-state levels of mitochondrial mRNAs, rRNAs and tRNAs, normalized to the *rp49* transcript levels, in 6-day-old adults of the *Lrpprc2*RNAi#2 line. (E) Quantification of northern blots shown in panel D. Error bars indicate mean ± 1 SD. Student's t-test was applied, $^{*}P < 0.05$, $^{**}P < 0.01$, $^{***}P < 0.001$. See also Supplementary Figures S3 and S4.

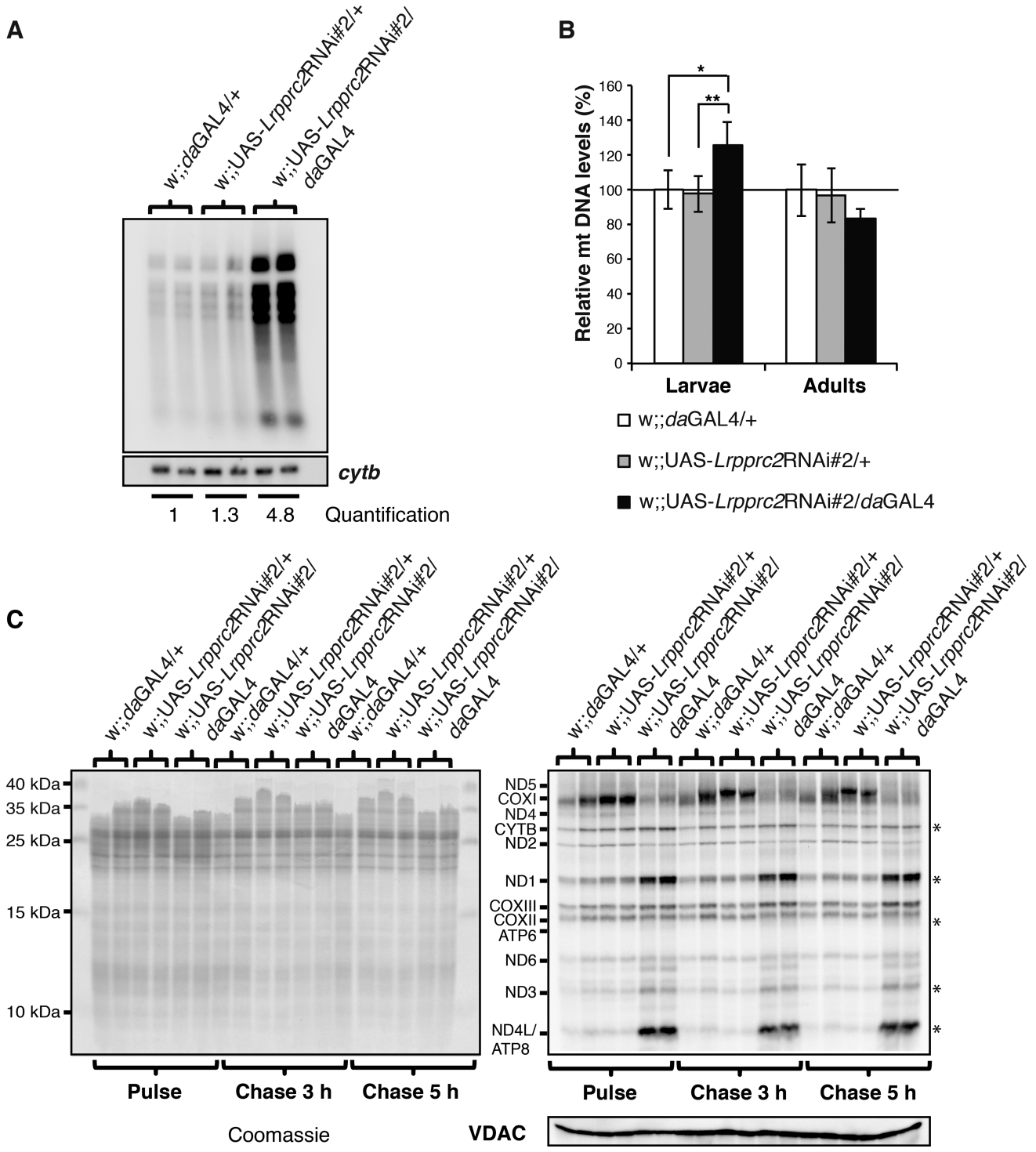

Figure 7. Analysis of mtDNA levels, *de novo* transcription and *in organello* translation. (A) Mitochondrial *de novo* transcription performed in isolated mitochondria from third-instar larvae of the *Lrpprc2*RNAi#2 line. *De novo* synthesized mitochondrial transcripts were labeled with α-^{32}P-dUTP and the *cytB* transcript detected by northern blot analyses was used as loading control, given that its steady-state levels were not different in *DmLrpprc2* KD and control individuals. Quantification of *de novo* transcription was performed by normalizing the profile of each lane to the *cytb* mRNA steady-state levels. The values reported for each genotype correspond to the average of two replicates. (B) qPCR analyses of steady-state levels of mtDNA in control (white and gray bars) and *DmLrpprc2* KD (black bars) third-instar larvae or 6-day-old adults of the *Lrpprc2*RNAi#2 line ($n = 4$–5). Error bars indicate mean ± 1 SD. Student's *t*-test was applied, $^{*}P < 0.05$, $^{**}P < 0.01$, $^{***}P < 0.001$. (C) Mitochondrial *in organello* translation performed on mitochondrial protein extracts from third-instar larvae of the *Lrpprc2*RNAi#2 line. Samples were collected 1 h after ^{35}S-methionine-labeling (pulse, right panel, left side) or 3 and 5 h after cold methionine addition (chase, right panel, right side) and separated in standard SDS-PAGE gels. Loading controls are provided by Coomassie staining to assess the total mitochondrial protein content per sample (left panel) and western blot analysis of VDAC protein levels in mitochondrial protein extracts collected after pulse and chase experiments. Asterisks mark the polypeptides whose levels are increased in DmLRPPRC2 KD samples compared to controls.

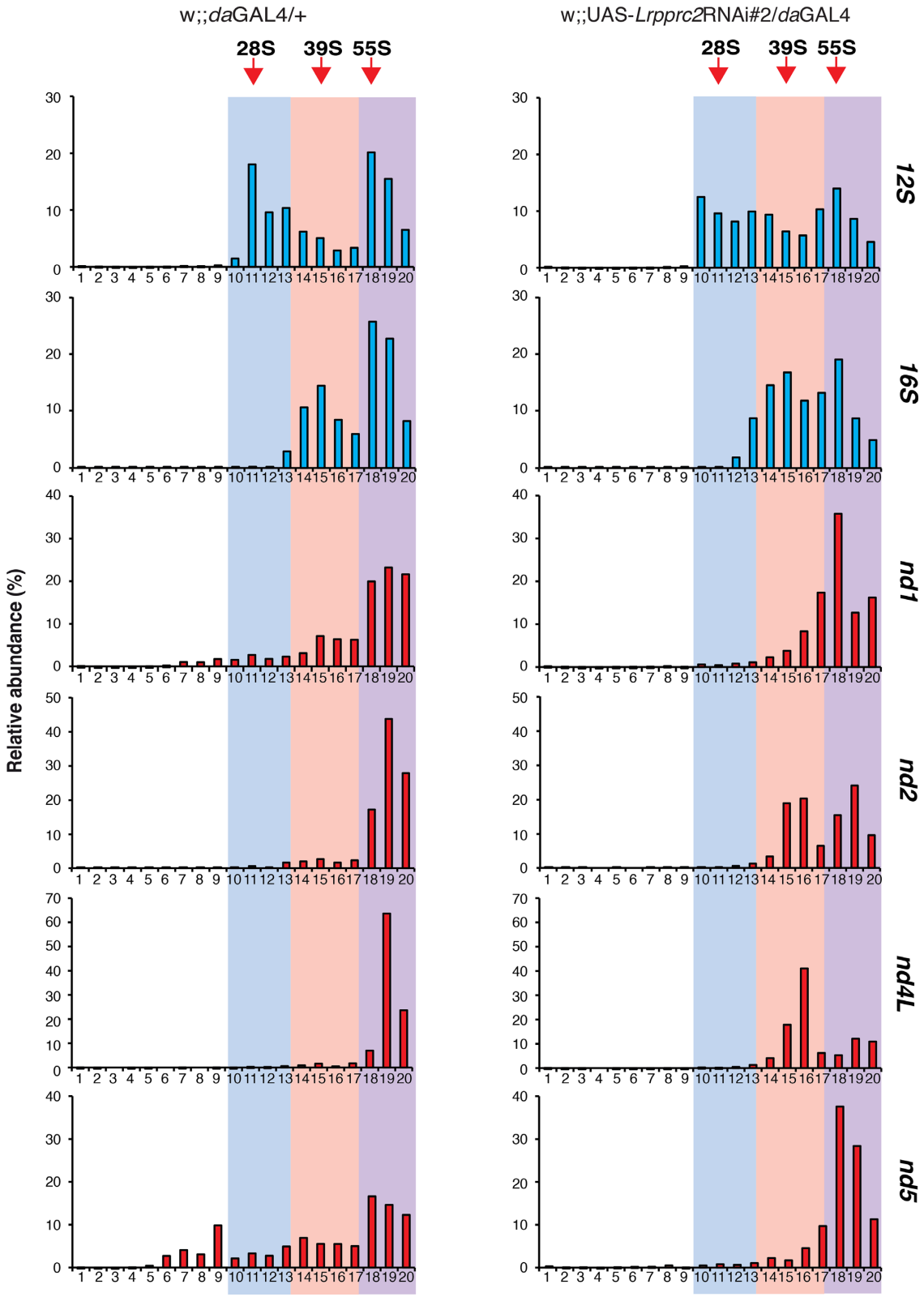

Figure 8. The interaction between mRNAs and the ribosome, as determined by sucrose density gradients. Mitochondrial RNAs were loaded on the top of a sucrose density gradient to assess the co-migration with the ribosome. Mitochondrial lysates from control (left side) and *DmLrpprc2* KD (right side) third-instar larvae of the *Lrpprc2*RNAi#2 line were analyzed. Mitochondrial transcripts were quantified through qRT-PCR analyses by using TaqMan or SYBR probes. The relative RNA abundance in each fraction is represented as the percentage relative to the total RNA abundance in the 20 fractions. The small (28S) ribosomal subunit, the large (39S) ribosomal subunit and the assembled (55S) ribosome are indicated by arrows. The *12S* rRNA sedimentation profile was used as marker for the migration of the 28S and the 55S ribosome particles. The *16S* rRNA sedimentation profile was used as a marker for the migration of the 39S and 55S ribosome particles. See also Supplementary Figure S5.

different analyzed mRNAs displayed a predominant sedimentation peak, which was co-migrating with the 55S ribosome. In control samples, we also observed that a fraction of mRNAs was migrating with the 39S ribosomal subunit (*nd1*, *nd5*) or were present in an extra-ribosomal pool (particularly evident for *nd5*) at the top of the gradient in fractions 6–9 (Figure 8, left panels). In contrast, the profiles of the *DmLrpprc2* KD samples showed that the proportion of mRNAs co-migrating with the 39S ribosomal subunit was much increased (*nd2, nd4L*) and in other cases the extra-ribosomal mRNA pool was decreased (*nd5*) (Figure 8, right panels). For some other mRNAs (*nd3*, *nd6*, *cytb*, *coxI*, *coxIII*, *atp6*) the migration pattern was very similar between control and *DmLrpprc2* KD samples (Supplementary Figure S5).

The results from analyses of *DmLrpprc2* KD larvae by using *de novo* translation (Figure 7C) and sucrose gradient sedimentation (Figure 8) assays show a misregulated translation. Some transcripts abnormally interact with the ribosomal components if DmLRPPRC2 is depleted and this is the likely cause of the observed uncoordinated and misregulated translation with dramatically increased or decreased synthesis of some polypeptides. To conclude, these findings suggest a role for DmLRPPRC2 as a coordinator of mitochondrial translation possibly by regulation of the access of newly synthesized transcripts to the mitochondrial ribosomes.

DmLRPPRC2 associates with DmSLIRP2

We generated flies expressing a FLAG-tagged version of DmLRPPRC2 and performed five FLAG-protein immunoprecipitation experiments on mitochondrial extracts from larval samples. As a control we used mitochondrial extracts from samples overexpressing the DmLRPPRC2 protein without a FLAG tag. We found in three out of five replicates that DmLRPPRC2 was bound to a protein annotated as CG8021, which corresponds to one out of the two stem-loop interacting RNA binding protein (SLIRP) homologs in flies and that we renamed DmSLIRP2 (Table 2). The absence of DmSLIRP2 peptides in two experiments is likely explained by the small size of the protein (10.3 kDa) limiting the number of detectable peptides. No binding was detected to the other SLIRP homolog annotated as CG33714 and here named as DmSLIRP1. In order to verify the specificity of the immunoprecipitation, the presence of DmLRPPRC2-FLAG and non-FLAG-tagged DmLRPPRC2 protein was analyzed by western blots at different stages of the procedure (Supplementary Figure S6). These results show that DmLRPPRC2 interacts with DmSLIRP2. This finding is consistent with previous reports in mammals showing that LRPPRC interacts with SLIRP (7,34,35).

DISCUSSION

The *in vivo* role for human *LRPPRC* has attracted a lot of attention as mutations in this gene cause a profound oxidative phosphorylation deficiency and a severe infantile form of the neurodegenerative Leigh syndrome. Studies of LRPPRC and DmLRPPRC1, the mouse and fly orthologs of human HsLRPPRC, have shown that these proteins are localized to mitochondria where they control mRNA stability, mRNA polyadenylation and regulation of mitochondrial translation (6,7,36). Unexpectedly, we show here that the fruit fly contains also a *LRPPRC* co-ortholog, which we denote *DmLrpprc2*. Downregulation of *DmLrpprc2* expression has no major effect on mRNA stability or maturation, including polyadenylation, but seems to lead to loss of proper coordination of mitochondrial translation (Table 3). When *DmLrpprc2* is downregulated, some mitochondrial mRNAs no longer preferentially interact with the fully assembled mitochondrial ribosome but are also found increasingly associated with the free 39S subunit and the extra-ribosomal pool of some transcripts disappears. Furthermore, if DmLRPPRC2 is depleted, mitochondrial translation is highly increased for some polypeptides and strongly decreased for other ones, leading to impaired oxidative phosphorylation. The role of DmLRPPRC2 therefore seems to be to make sure that the mitochondrial transcripts enter the ribosome in a controlled fashion to achieve proper temporal control of translation. A possible model is that the DmLRPPRC2 protein is involved in a checkpoint step to allow a coordination of the transcription and translation processes.

Interestingly, the levels of DmLRPPRC1 are increased when DmLRPPRC2 is depleted and *vice versa*, showing that the substantial phenotypes caused by downregulated expression of either *DmLrpprc1* or *DmLrpprc2* cannot be rescued by the overexpression of the paralog protein. Therefore, the functions of the two *Drosophila* LRPPRC orthologs are not overlapping and DmLRPPRC2 has a novel important role in mitochondrial translation.

It is likely the *DmLrpprc1* has undergone a gene duplication event to generate the *DmLrpprc2* gene, which subsequently has evolved a new and different essential function in mitochondrial translation. There are other examples of similar evolutionary processes in flies, e.g. the *Drosophila timeless1* (*tim1*) and *timeless2* (*tim2*) genes are both homologous to a single mammalian gene named *timeout*. It has been proposed that *tim1* originated from a duplication event of the *tim2* locus occurring around the time of the Cambrian explosion (48). Whereas *tim1* is a key component of the *Drosophila* circadian clock (49,50), *tim2* has other distinct roles involving regulation of chromosome stability during development and circadian photoreception in adult flies (48,51). The two paralogs have thus evolved distinct and non-overlapping functions, however, they are still weakly functionally related as both have roles in the circadian system (48).

Mammalian LRPPRC interacts with a small 12 kDa protein called SLIRP (7,34,35). The complex between LRPPRC and SLIRP is RNA-dependent (7) and can counteract SUV3- and PNPase-mediated transcript degradation (35). Interestingly, the *Drosophila melanogaster* genome harbors two *Slirp* genes (Flybase annotation numbers: #CG33714 and #CG8021) that are predicted to recognize and bind RNA (http//:flybase.org). It is unclear if there is an evolutionary link between duplication events that generated *DmLrpprc1* and *DmLrpprc2* on the one hand, and the two *Slirp* genes on the other hand. We observed that DmLRPPRC2 interacts with one out of the two SLIRP homologs in *Drosophila*, here named DmSLIRP2 (#CG8021). Fur-

Table 2. Mass spectrometry analysis of DmLRPPRC2 and DmSLIRP2 interaction

Replicate (*n*)	DmLRPPRC2-FLAG (120.1 kDa)			DmSLIRP2 (CG8021; 10.3 kDa)		
	Peptides	Coverage (%)	Peptides in negative control	Peptides	Coverage (%)	Peptides in negative control
1	34	35.35	0	3	47.25	0
2	51	44.68	0	-	-	0
3	76	57.5	14	4	58.2	0
4	72	61.7	2	-	-	0
5	75	60.3	0	1	14.3	0

Table 3. Similarities and differences between DmLRPPRC1 and DmLRPPRC2

Characteristics	DmLRPPRC1 KD	DmLRPPRC2 KD
essential factor	yes	yes
mtDNA levels	normal (adults) or slightly ↑ (larvae)	normal (adults) or slightly ↑ (larvae)
mRNA steady-state levels	↓	generally normal or ↑
poly-A tail length	↓ (except *cytb* and *atp8/6*)	normal
de novo transcription	↑	↑
de novo translation	↑ (normal for CYTB and ATP6)	normal or ↑ or ↓
decreased stability of newly synthesized peptides	yes (only for COXII and a product above ND1)	no
OXPHOS dysfunction	yes (Complex I and IV most affected)	yes (Complex I, IV and V most affected)

ther investigations are required to elucidate the molecular function of this interaction.

Several findings suggest that complex I is the component of the oxidative phosphorylation that is most affected when DmLRPPRC2 levels are decreased: (*i*) The in-gel activity and steady-state levels of assembled complex I are decreased on BN-PAGE. (*ii*) The complex I enzyme activity and its contribution to mitochondrial respiration are decreased. (*iii*) Most of the mtDNA-encoded complex I subunits are synthesized at dramatically increased levels. (*iv*) Several mtDNA transcripts encoding complex I subunits are abnormally interacting with the ribosome. The severe effects on complex I could reflect the fact that this is the largest and most complicated of the respiratory chain enzyme complexes, which makes it more sensitive to perturbations. This is also consistent with the observation that complex I is commonly involved in human mitochondrial diseases (52).

Interestingly, the distinct mitochondrial roles of DmLRPPRC1 and DmLRPPRC2 are congruent with the functional classification of PPR proteins in *Schizosaccharomyces pombe*, where two main functional classes have been proposed: (i) regulation of mitochondrial transcript stability and (ii) regulation of mitochondrial translation (53). A similar functional organization of PPR proteins has also been proposed for *Saccharomyces cerevisiae* (22).

Despite the massive increase of *de novo* mitochondrial transcription, we mainly observed an increase of the steady-state levels of some tRNAs, whereas the steady-state levels of the mitochondrial mRNAs were not generally affected in the DmLRPPRC2 KD. Similar patterns have been observed in mice with a conditional knockout of *Tfb1m*, which is required for ribosomal biogenesis. These mice have a massive increase of mitochondrial *de novo* transcription, increased levels of tRNAs and normal levels of most mRNAs (45). These patterns are likely explained by post-transcriptional mechanisms regulating the steady-state levels of mRNAs, whereas tRNAs do not seem to have this type of regulation of their steady-state levels.

There are many examples that loss of specific genes causes a global reduction in mitochondrial translation, e.g. MTERF3 (5), MTERF4 (47), TFB1M (45), NSUN4 (54), nitric oxide associated-1 (NOA1) (55) or the recently characterized coiled-coil-helix-coiled-coil-helix domain containing protein 1 (CHCHD1 or MRPS37), Aurora kinase A interacting protein 1 (AURKAIP1 or MRPS38) and CR-6 interacting factor 1 (CRIF1 or MRPL59) (56). However, there are only a few examples where downregulated expression of specific genes causes increased mitochondrial translation. One example is DmLRPPRC1, whose downregulation leads to a general overproduction of mitochondrial polypeptides except for CYTB and ATP6 (6). Another example is the Ppr5 protein, one of the 10 PPR proteins in *Schizosaccharomyces pombe*, that is a general negative regulator of mitochondrial translation (53). Another example is the mammalian PTCD1, which has been reported to limit the mitochondrial protein synthesis by specifically lowering the availability of the two tRNAs carrying leucine in their aminoacylated form (27). In this study, we observed that mitochondrial *de novo* translation is strongly increased for some mitochondrial peptides, and unchanged or even severely decreased for other ones in DmLRPPRC2 KD larval samples. In particular, the decreased synthesis of ND2/ND4 and of COXI are consistent with the defective complex I and complex IV activities.

Unfortunately, with the fly model the investigation on the assembly state of the ribosomes in sucrose gradient experiments is limited by the unavailability of antibodies recognizing mitochondrial ribosome components. However, previous studies from our group have demonstrated that the *12S* and *16S* rRNAs can be considered good markers for mitochondrial ribosomal abundance and assembly (5,7). Both qRT-PCR and northern blots show that the steady-state levels of *12S* and *16S* rRNAs are not changed in DmLRPPRC2 KD larvae in comparison with controls. These results

show that the total ribosome subunit abundance is similar in control and DmLRPPRC2 KD larvae. Furthermore, analysis of the ribosomal assembly status show that a high proportion of the subunits is present in monosomes in both control and DmLRPPRC2 KD larvae (Figure 8).

To conclude, we report here that the *Drosophila* PPR protein DmLRPPRC2 is primarily localized to mitochondria, where it interacts with DmSLIRP2 and seems to have an essential function in coordinating translation, likely by controlling the entrance of mRNAs into the mitochondrial ribosomes. Surprisingly, unlike its homologs, DmLRPPRC1 in *Drosophila* and LRPPRC in mammals, it does not influence RNA metabolism processes, such as transcript stability and polyadenylation. Thus, DmLRPPRC2 has a specific and distinct role with respect to its paralog DmLRPPRC1. It is interesting to note that if DmLRPPRC2 is depleted, mitochondrial synthesis of some proteins is dramatically increased whereas the synthesis of other proteins is decreased, despite largely normal steady-state levels of mRNAs. We therefore propose that DmLRPPRC2 interacts with mRNAs to present them in an orderly fashion to the ribosome.

SUPPLEMENTARY DATA

Supplementary Data are available at NAR Online.

ACKNOWLEDGEMENT

We would like to thank Professor P.M. MacDonald, Stanford University, for providing the polyclonal rat antiserum against DmLRPPRC1.

FUNDING

European Research Council (ERC) [268897]; Deutsche Forschungsgemeinschaft [SFB829]; Swedish Research Council [K2014–66X-12197–18–3 to N.-G.L.]. Funding for open access charge: ERC [268897].
Conflict of interest statement. None declared.

REFERENCES

1. Boore,J.L. (1999) Animal mitochondrial genomes. *Nucleic Acids Res.*, **27**, 1767–1780.
2. Oliveira,M.T., Garesse,R. and Kaguni,L.S. (2010) Animal models of mitochondrial DNA transactions in disease and ageing. *Exp. Gerontol.*, **45**, 489–502.
3. Wallace,D.C. (2005) A mitochondrial paradigm of metabolic and degenerative diseases, aging, and cancer: a dawn for evolutionary medicine. *Annu. Rev. Genet.*, **39**, 359–407.
4. Falkenberg,M., Larsson,N.G. and Gustafsson,C.M. (2007) DNA replication and transcription in mammalian mitochondria. *Annu. Rev. Biochem.*, **76**, 679–699.
5. Wredenberg,A., Lagouge,M., Bratic,A., Metodiev,M.D., Spåhr,H., Mourier,A., Freyer,C., Ruzzenente,B., Tain,L., Grönke,S. *et al.* (2013) MTERF3 regulates mitochondrial ribosome biogenesis in invertebrates and mammals. *PLoS Genet.*, **9**, e1003178.
6. Bratic,A., Wredenberg,A., Grönke,S., Stewart,J.B., Mourier,A., Ruzzenente,B., Kukat,C., Wibom,R., Habermann,B., Partridge,L. *et al.* (2011) The bicoid stability factor controls polyadenylation and expression of specific mitochondrial mRNAs in *Drosophila melanogaster*. *PLoS Genet.*, **7**, e1002324.
7. Ruzzenente,B., Metodiev,M.D., Wredenberg,A., Bratic,A., Park,C.B., Cámara,Y., Milenkovic,D., Zickermann,V., Wibom,R., Hultenby,K. *et al.* (2011) LRPPRC is necessary for polyadenylation and coordination of translation of mitochondrial mRNAs. *EMBO J.*, **31**, 443–456.
8. Small,I.D. and Peeters,N. (2000) The PPR motif - a TPR-related motif prevalent in plant organellar proteins. *Trends Biochem. Sci.*, **25**, 46–47.
9. Schmitz-Linneweber,C. and Small,I. (2008) Pentatricopeptide repeat proteins: a socket set for organelle gene expression. *Trends Plant Sci.*, **13**, 663–670.
10. Fujii,S. and Small,I. (2011) The evolution of RNA editing and pentatricopeptide repeat genes. *New Phytol.*, **191**, 37–47.
11. Lurin,C., Andrés,C., Aubourg,S., Bellaoui,M., Bitton,F., Bruyère,C., Caboche,M., Debast,C., Gualberto,J., Hoffmann,B. *et al.* (2004) Genome-wide analysis of *Arabidopsis* pentatricopeptide repeat proteins reveals their essential role in organelle biogenesis. *Plant Cell*, **16**, 2089–2103.
12. Rivals,E., Bruyère,C., Toffano-Nioche,C. and Lecharny,A. (2006) Formation of the *Arabidopsis* pentatricopeptide repeat family. *Plant Physiol.*, **141**, 825–839.
13. O'Toole,N., Hattori,M., Andres,C., Iida,K., Lurin,C., Schmitz-Linneweber,C., Sugita,M. and Small,I. (2008) On the expansion of the pentatricopeptide repeat gene family in plants. *Mol. Biol. Evol.*, **25**, 1120–1128.
14. Shikanai,T. and Fujii,S. (2013) Function of PPR proteins in plastid gene expression. *RNA Biol.*, **10**, 1446–1456.
15. Filipovska,A. and Rackham,O. (2013) Pentatricopeptide repeats: modular blocks for building RNA-binding proteins. *RNA Biol.*, **10**, 1426–1432.
16. Zehrmann,A., Verbitskiy,D., Härtel,B., Brennicke,A. and Takenaka,M. (2011) PPR proteins network as site-specific RNA editing factors in plant organelles. *RNA Biol.*, **8**, 67–70.
17. Barkan,A., Rojas,M., Fujii,S., Yap,A., Chong,Y.S., Bond,C.S. and Small,I. (2012) A combinatorial amino acid code for RNA recognition by pentatricopeptide repeat proteins. *PLoS Genet.*, **8**, e1002910.
18. Kobayashi,K., Kawabata,M., Hisano,K., Kazama,T., Matsuoka,K., Sugita,M. and Nakamura,T. (2011) Identification and characterization of the RNA binding surface of the pentatricopeptide repeat protein. *Nucleic Acids Res.*, **40**, 2712–2723.
19. Yagi,Y., Hayashi,S., Kobayashi,K., Hirayama,T. and Nakamura,T. (2013) Elucidation of the RNA recognition code for pentatricopeptide repeat proteins involved in organelle RNA editing in plants. *PLoS One*, **8**, e57286.
20. Yin,P., Li,Q., Yan,C., Liu,Y., Liu,J., Yu,F., Wang,Z., Long,J., He,J., Wang,H.W. *et al.* (2013) Structural basis for the modular recognition of single-stranded RNA by PPR proteins. *Nature*, **504**, 168–171.
21. Liu,G., Mercer,T.R., Shearwood,A.M., Siira,S.J., Hibbs,M.E., Mattick,J.S., Rackham,O. and Filipovska,A. (2013) Mapping of mitochondrial RNA-protein interactions by digital RNase footprinting. *Cell Rep.*, **5**, 839–848.
22. Herbert,C.J., Golik,P. and Bonnefoy,N. (2013) Yeast PPR proteins, watchdogs of mitochondrial gene expression. *RNA Biol.*, **10**, 1477–1494.
23. Aphasizhev,R. and Aphasizheva,I. (2013) Emerging roles of PPR proteins in trypanosomes: switches, blocks, and triggers. *RNA Biol.*, **10**, 1495–1500.
24. Rackham,O. and Filipovska,A. (2012) The role of mammalian PPR domain proteins in the regulation of mitochondrial gene expression. *Biochim. Biophys. Acta*, **1819**, 1008–1016.
25. Lightowlers,R.N. and Chrzanowska-Lightowlers,Z.M. (2013) Human pentatricopeptide proteins: only a few and what do they do? *RNA Biol.*, **10**, 1433–1438.
26. Ringel,R., Sologub,M., Morozov,Y.I., Litonin,D., Cramer,P. and Temiakov,D. (2011) Structure of human mitochondrial RNA polymerase. *Nature*, **478**, 269–273.
27. Rackham,O., Davies,S.M., Shearwood,A.M., Hamilton,K.L., Whelan,J. and Filipovska,A. (2009) Pentatricopeptide repeat domain protein 1 lowers the levels of mitochondrial leucine tRNAs in cells. *Nucleic Acids Res.*, **37**, 5859–5867.
28. Sanchez,M.I., Mercer,T.R., Davies,S.M., Shearwood,A.M., Nygård,K.K., Richman,T.R., Mattick,J.S., Rackham,O. and Filipovska,A. (2011) RNA processing in human mitochondria. *Cell Cycle*, **10**, 2904–2916.
29. Xu,F., Ackerley,C., Maj,M.C., Addis,J.B., Levandovskiy,V., Lee,J., Mackay,N., Cameron,J.M. and Robinson,B.H. (2008) Disruption of a mitochondrial RNA-binding protein gene results in decreased cytochrome b expression and a marked reduction in

ubiquinol-cytochrome c reductase activity in mouse heart mitochondria. *Biochem. J.*, **416**, 15–26.
30. Davies,S.M., Rackham,O., Shearwood,A.M., Hamilton,K.L., Narsai,R., Whelan,J. and Filipovska,A. (2009) Pentatricopeptide repeat domain protein 3 associates with the mitochondrial small ribosomal subunit and regulates translation. *FEBS Lett.*, **583**, 1853–1858.
31. Davies,S.M., Lopez Sanchez,M.I., Narsai,R., Shearwood,A.M., Razif,M.F., Small,I.D., Whelan,J., Rackham,O. and Filipovska,A. (2012) MRPS27 is a pentatricopeptide repeat domain protein required for the translation of mitochondrially encoded proteins. *FEBS Lett.*, **586**, 3555–3561.
32. Holzmann,J., Frank,P., Löffler,E., Bennett,K.L., Gerner,C. and Rossmanith,W. (2008) RNase P without RNA: identification and functional reconstitution of the human mitochondrial tRNA processing enzyme. *Cell*, **135**, 462–474.
33. Sterky,F.H., Ruzzenente,B., Gustafsson,C.M., Samuelsson,T. and Larsson,N.G. (2010) LRPPRC is a mitochondrial matrix protein that is conserved in metazoans. *Biochem. Biophys. Res. Commun.*, **398**, 759–764.
34. Sasarman,F., Brunel-Guitton,C., Antonicka,H., Wai,T., Shoubridge,E.A. and LSFC Consortium. (2010) LRPPRC and SLIRP interact in a ribonucleoprotein complex that regulates posttranscriptional gene expression in mitochondria. *Mol. Biol. Cell.*, **21**, 1315–1323.
35. Chujo,T., Ohira,T., Sakaguchi,Y., Goshima,N., Nomura,N., Nagao,A. and Suzuki,T. (2012) LRPPRC/SLIRP suppresses PNPase-mediated mRNA decay and promotes polyadenylation in human mitochondria. *Nucleic Acids Res.*, **40**, 8033–8047.
36. Harmel,J., Ruzzenente,B., Terzioglu,M., Spåhr,H., Falkenberg,M. and Larsson,N.G. (2013) The leucine-rich pentatricopeptide repeat-containing protein (LRPPRC) does not activate transcription in mammalian mitochondria. *J. Biol. Chem.*, **2288**, 15510–15519.
37. Mourier,A., Ruzzenente,B., Brandt,T., Kühlbrandt,W. and Larsson,N.G. (2014) Loss of LRPPRC causes ATP synthase deficiency. *Hum. Mol. Genet.*, **23**, 2580–2592.
38. Merante,F., Petrova-Benedict,R., MacKay,N., Mitchell,G., Lambert,M., Morin,C., De Braekeleer,M., Laframboise,R., Gagné,R. and Robinson,B.H. (1993) A biochemically distinct form of cytochrome oxidase (COX) deficiency in the Saguenay-Lac-Saint-Jean region of Quebec. *Am. J. Hum. Genet.*, **53**, 481–487.
39. Xu,F., Morin,C., Mitchell,G., Ackerley,C. and Robinson,B.H. (2004) The role of the LRPPRC (leucine-rich pentatricopeptide repeat cassette) gene in cytochrome oxidase assembly: mutation causes lowered levels of COX (cytochrome c oxidase) I and COX III mRNA. *Biochem. J.*, **382**, 331–336.
40. Debray,F.G., Morin,C., Janvier,A., Villeneuve,J., Maranda,B., Laframboise,R., Lacroix,J., Decarie,J.C., Robitaille,Y., Lambert,M. *et al.* (2011) LRPPRC mutations cause a phenotypically distinct form of Leigh syndrome with cytochrome c oxidase deficiency. *J. Med. Genet.*, **48**, 183–189.
41. Greene,J.C., Whitworth,A.J., Kuo,I., Andrews,L.A., Feany,M.B. and Pallanck,L.J. (2003) Mitochondrial pathology and apoptotic muscle degeneration in *Drosophila* parkin mutants. *Proc. Natl. Acad. Sci. U.S.A.*, **100**, 4078–4083.
42. Cox,B. and Emili,A. (2006) Tissue subcellular fractionation and protein extraction for use in mass-spectrometry-based proteomics. *Nat. Protoc.*, **1**, 1872–1878.
43. Wredenberg,A., Wibom,R., Wilhelmsson,H., Graff,C., Wiener,H.H., Burden,S.J., Oldfors,A., Westerblad,H. and Larsson,N.G. (2002) Increased mitochondrial mass in mitochondrial myopathy mice. *Proc. Natl. Acad. Sci. U.S.A.*, **99**, 15066–15071.
44. Shannon,M.F. and Duke,E.J. (1985) Comparison of mitochondrial and cytoplasmic ribosomal-proteins in *Drosophila*. *Comparat. Biochem. Phys. B-Biochem. Mol. Biol.*, **81**, 683–686.
45. Metodiev,M.D., Lesko,N., Park,C.B., Cámara,Y., Shi,Y., Wibom,R., Hultenby,K., Gustafsson,C.M. and Larsson,N.G. (2009) Methylation of *12S* rRNA is necessary for in vivo stability of the small subunit of the mammalian mitochondrial ribosome. *Cell Metab.*, **9**, 386–397.
46. Brand,A.H. and Perrimon,N. (1993) Targeted gene expression as a means of altering cell fates and generating dominant phenotypes. *Development*, **118**, 401–415.
47. Cámara,Y., Asin-Cayuela,J., Park,C.B., Metodiev,M.D., Shi,Y., Ruzzenente,B., Kukat,C., Habermann,B., Wibom,R., Hultenby,K. *et al.* (2011) MTERF4 regulates translation by targeting the methyltransferase NSUN4 to the mammalian mitochondrial ribosome. *Cell Metab.*, **13**, 527–539.
48. Benna,C., Bonaccorsi,S., Wülbeck,C., Helfrich-Förster,C., Gatti,M., Kyriacou,C.P., Costa,R. and Sandrelli,F. (2010) *Drosophila timeless2* is required for chromosome stability and circadian photoreception. *Curr. Biol.*, **20**, 346–352.
49. Suri,V., Lanjuin,A. and Rosbash,M. (1999) TIMELESS-dependent positive and negative autoregulation in the *Drosophila* circadian clock. *EMBO J.*, **18**, 675–686.
50. Ozkaya,O. and Rosato,E. (2012) The circadian clock of the fly: a neurogenetics journey through time. *Adv. Genet.*, **77**, 79–123.
51. Benna,C., Scannapieco,P., Piccin,A., Sandrelli,F., Zordan,M., Rosato,E., Kyriacou,C.P., Valle,G. and Costa,R. (2000) A second *timeless* gene in *Drosophila* shares greater sequence similarity with mammalian *tim*. *Curr. Biol.*, **10**, R512–R513.
52. Hoefs,S.J., Rodenburg,R.J., Smeitink,J.A. and van den Heuvel,L.P. (2012) Molecular base of biochemical complex I deficiency. *Mitochondrion*, **12**, 520–532.
53. Kühl,I., Dujeancourt,L., Gaisne,M., Herbert,C.J. and Bonnefoy,N. (2011) A genome wide study in fission yeast reveals nine PPR proteins that regulate mitochondrial gene expression. *Nucleic Acids Res.*, **39**, 8029–8041.
54. Metodiev,M.D., Spåhr,H., Loguercio Polosa,P., Meharg,C., Becker,C., Altmueller,J., Habermann,B., Larsson,N.G. and Ruzzenente,B. (2014) NSUN4 is a dual function mitochondrial protein required for both methylation of *12S* rRNA and coordination of mitoribosomal assembly. *PLOS Genet.*, **10**, e1004110.
55. Kolanczyk,M., Pech,M., Zemojtel,T., Yamamoto,H., Mikula,I., Calvaruso,M.A., van den Brand,M., Richter,R., Fischer,B., Ritz,A. *et al.* (2011) NOA1 is an essential GTPase required for mitochondrial protein synthesis. *Mol. Biol. Cell*, **22**, 1–11.
56. Koc,E.C., Cimen,H., Kumcuoglu,B., Abu,N., Akpinar,G., Haque,M.E., Spremulli,L.L. and Koc,H. (2013) Identification and characterization of CHCHD1, AURKAIP1, and CRIF1 as new members of the mammalian mitochondrial ribosome. *Front. Physiol.*, **4**, 183.